

MAY 13 1997

# SANDIA REPORT

SAND97-0915 • UC-404

Unlimited Release

Printed May 1997

## Structural Mechanisms of Nonplanar Hemes in Proteins

RECEIVED

MAY 27 1997

OSTI

John A. Shelnut

DISTRIBUTION OF THIS DOCUMENT IS UNLIMITED

Prepared by  
Sandia National Laboratories  
Albuquerque, New Mexico 87185 and Livermore, California 94550

Sandia is a multiprogram laboratory operated by Sandia Corporation, a Lockheed Martin Company, for the United States Department of Energy under Contract DE-AC04-94AL85000.

Approved for public release; distribution is unlimited.

MASTER



Sandia National Laboratories

A handwritten signature or mark at the bottom right of the page.

Issued by Sandia National Laboratories, operated for the United States Department of Energy by Sandia Corporation.

**NOTICE:** This report was prepared as an account of work sponsored by an agency of the United States Government. Neither the United States Government nor any agency thereof, nor any of their employees, nor any of their contractors, subcontractors, or their employees, makes any warranty, express or implied, or assumes any legal liability or responsibility for the accuracy, completeness, or usefulness of any information, apparatus, product, or process disclosed, or represents that its use would not infringe privately owned rights. Reference herein to any specific commercial product, process, or service by trade name, trademark, manufacturer, or otherwise, does not necessarily constitute or imply its endorsement, recommendation, or favoring by the United States Government, any agency thereof, or any of their contractors or subcontractors. The views and opinions expressed herein do not necessarily state or reflect those of the United States Government, any agency thereof, or any of their contractors.

Printed in the United States of America. This report has been reproduced directly from the best available copy.

Available to DOE and DOE contractors from  
Office of Scientific and Technical Information  
P.O. Box 62  
Oak Ridge, TN 37831

Prices available from (615) 576-8401, FTS 626-8401

Available to the public from  
National Technical Information Service  
U.S. Department of Commerce  
5285 Port Royal Rd  
Springfield, VA 22161

NTIS price codes  
Printed copy: A03  
Microfiche copy: A01

## Structural Mechanisms of Nonplanar Hemes in Proteins

John A. Shelnutt  
Catalysis and Chemical Technologies Department  
Sandia National Laboratories  
P. O. Box 5800  
Albuquerque, NM 87185-0710

### Abstract

The objective is to assess the occurrence of nonplanar distortions of hemes and other tetrapyrroles in proteins and to determine the biological function of these distortions. Recently, these distortions were found by us to be conserved among proteins belonging to a functional class. Conservation of the conformation of the heme indicates a possible functional role. Researchers have suggested possible mechanisms by which heme distortions might influence biological properties; however, no heme distortion has yet been shown conclusively to participate in a structural mechanism of hemoprotein function. The specific aims of the proposed work are: (1) to characterize and quantify the distortions of the hemes in all of the more than 300 hemoprotein X-ray crystal structures in terms of displacements along the lowest-frequency normal coordinates, (2) to determine the structural features of the protein component that generate and control these nonplanar distortions by using spectroscopic studies and molecular-mechanics calculations for the native proteins, their mutants and heme-peptide fragments, and model porphyrins, (3) to determine spectroscopic markers for the various types of distortion, and, finally, (4) to discover the functional significance of the nonplanar distortions by correlating function with porphyrin conformation for proteins and model porphyrins. The normal structural decomposition (NSD) method is crucial to successfully achieving these goals. NSD is a new computational procedure for quantifying the distortions of porphyrins, especially in protein crystal structures. Using the NSD procedure, the heme groups in X-ray structures are found to show different conserved distortions for different functional classes of proteins. The NSD method in combination with molecular mechanics and spectroscopic studies provide the means for discovering the structural mechanisms that cause the different types of distortion. Understanding the influence of heme nonplanarity on the function of heme proteins has substantial significance for understanding allosteric control mechanisms in biology and for the purpose of developing biomimes for use in health-related and commercial processes.

Type the name of the principal investigator/program director at the top of each printed page and each continuation page. (For type specifications, see instructions on page 6.)

## RESEARCH GRANT TABLE OF CONTENTS

	Page Numbers
Table of Contents .....	<u>1</u>
 <b>Research Plan</b>	
a. Specific Aims .....	2
b. Background and Significance .....	3
c. Preliminary Studies/Progress Report..	6
d. Research Design and Methods .....	15
<i>(Items a-d: not to exceed 25 pages*)...</i>	

## a. Specific Aims

Our ultimate goal is to determine the functional significance of nonplanar heme distortions in hemoproteins. It has been recognized for about 10 years that the hemes in many hemoproteins are highly distorted from planarity and that these nonplanar distortions might play a role in their biological function.<sup>1-4</sup> In related photosynthetic proteins, nonplanar distortions have been suggested to influence the redox properties of chlorophyll pigments, with consequent effects on electron-transfer rates in photosynthetic reaction centers and antennae complexes.<sup>1a,b</sup> More recently, by using a new method for characterizing and quantifying these distortions, our group has found that these distortions are often of different types for proteins with different functions, and the types of distortion are conserved for proteins belonging to the same functional class.<sup>5,6</sup> This suggests even more strongly that the biological function of hemoproteins might be modulated by protein control over the conformation of the heme prosthetic group. The importance of the nonplanar distortions of the heme is also emphasized by recent studies of model nonplanar porphyrins showing, first, that hemes are expected to be nearly planar in absence of the protein moiety<sup>7</sup> and, second, that the nonplanar structure influences relevant chemical and photophysical properties (*e.g.*, axial ligand affinity, redox potentials, transition dipoles and energies).<sup>1-4,8-11</sup>

The first specific aim of the proposed work is to evaluate all of the 325 heme protein X-ray crystal structures in the Protein Data Bank using the newly developed normal structural decomposition (NSD) procedure.<sup>5,8,12</sup> This will quantify and characterize the heme conformational motifs present in the hemoproteins and the degree to which these motifs are maintained within functional classes of proteins. Already over 100 hemes of the proteins have been characterized with NSD and, in most cases, the nonplanar structures have been found to be characteristic of the specific protein types. The structural decomposition of all of the hemes in the Protein Data Bank will also delineate the effects of natural amino acid sequence variation, mutation, axial ligation, and other protein differences on the conformation of the heme.

Another aim is to relate the primary, secondary, and tertiary structure of the protein moiety to the particular conformation of the heme. In the case of the *c*-type cytochromes, a mechanism for producing the strong ruffling of the heme skeleton is suggested by the NSD results.<sup>5,6,12</sup> We expect that NSD characterization of the hemes in other proteins will lead to other hypotheses relating protein structure and heme conformation. Based on these hypotheses, spectroscopic and molecular modeling studies will be carried out to verify or disprove the structural mechanisms proposed. The methods to be used in these studies are illustrated by our preliminary results for nickel-reconstituted cytochrome *c* and nickel microperoxidase-11, in which a proposed mechanism of protein-heme interaction leading to the ruffling of the heme in the cytochromes *c* is tested.

Studies of model nonplanar porphyrins are also necessary to improve the ability of spectroscopic techniques to distinguish the types and magnitudes of distortion of the heme. Currently, resonance Raman spectroscopy allows one to distinguish the magnitude of nonplanar distortion but not the type (*e.g.*, doming, ruffling, saddling, etc.). In addition, at present it is unknown whether the relationship between Raman line frequencies and the magnitude of distortion varies with the type of distortion. Further improvements in the spectroscopic probes of porphyrin structure are another specific goal of the proposed work.

Molecular modeling studies coupled with the spectroscopic data and the NSD results provide critical insight into the possible mechanisms by which the surroundings of the porphyrin can induce various nonplanar distortions. A molecular mechanics force field has been developed and exhaustively validated experimentally for the prediction of porphyrin conformations.<sup>7,8,11,13-16</sup> The molecular modeling will provide information about the energetics of nonplanar distortions, aiding in the determination of their functional significance and structural origin.

Finally, the relationships between chemical function and heme structure will be directly examined in proteins and model porphyrin systems. For example, a series of porphyrins in which the magnitude of the nonplanarity is varied by changing the bulkiness of the peripheral substituents will be used to investigate the effect of each type of nonplanar distortion on axial ligation and other chemical properties. Such investigations will determine the magnitude of the effects induced by nonplanar distortion and the different ways in which nonplanar conformers can influence chemical properties. In the proteins, NSD results for heme proteins will be correlated to functional properties in as much as is possible. Also, protein function will be varied by mutation and by changing the pH and other solution properties, so that possible correlations with the spectroscopically-determined heme conformations can be ascertained.

## b. Background and Significance

*Structure-Function Relationships in Hemoproteins.* Since Warburg's work beginning over 70 years ago,<sup>17</sup> the heme proteins have been intensely investigated with the aim of determining the structural mechanisms controlling their varied biological functions. The major remaining questions concern the role of the protein in modulating the properties of the iron-porphyrin cofactor to yield the specific biological functions, *e.g.*, electron transfer (cytochromes), O<sub>2</sub> transport and storage (hemoglobin, myoglobin), respiration (cytochrome oxidase), or catalysis (peroxidase, monooxygenase, catalase). The immediate surroundings of the heme active site certainly have a dominant influence on function; in particular, axial coordination to the central iron atom, covalent attachment of the heme to the protein, and amino acid side chains in the immediate vicinity of the active site are all important. However, subtle influences on the structure of the active site are sometimes observed to modify the activity of the protein. For example, in the cytochromes the number, H-bonding interactions, conformations, and nature of the axial ligands appear to be of primary importance in governing the redox properties.<sup>18</sup> As another example, the hemes in hemoglobin have oxygen affinities that depend on whether the other hemes have O<sub>2</sub> bound as an axial ligand or not. Heme affinity differences in hemoglobin have been ascribed to subtle structural changes in axial coordination to the iron atom which are transmitted from one heme to the others through the protein's tertiary and quaternary structure.<sup>19</sup> It is also possible that conformational differences in the heme itself may influence the reactivity of heme proteins.

To arrive at a detailed structural understanding of the function of heme proteins requires a thorough knowledge of the various influences of structure on function. In many instances, the structure of the heme is ignored in the proposed structural mechanism. However, crystallographers have recently noted some highly

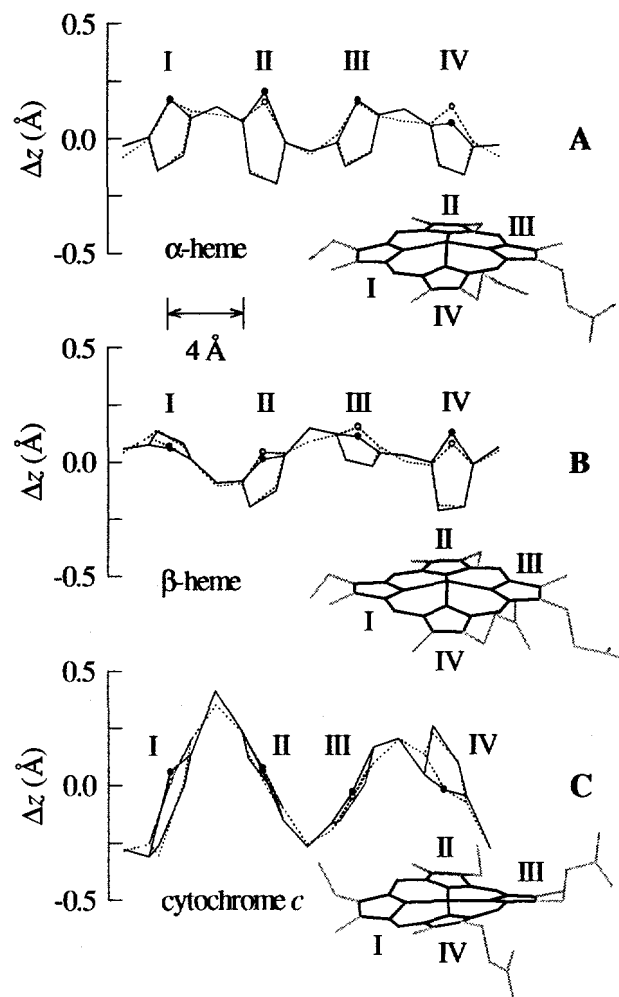


**Figure 1.** Linear displays of the hemes in the  $\alpha$  and  $\beta$  subunits of deoxyhemoglobin A and in cytochrome c isolated from yeast. The dotted lines represent the simulated structure obtained from a linear combination of displacements along only the lowest-frequency normal coordinate of each out-of-plane symmetry (vide infra).

**DISCLAIMER**

**Portions of this document may be illegible  
in electronic image products. Images are  
produced from the best available original  
document.**

distorted heme conformations occurring in X-ray structures of proteins.<sup>20</sup> And, since the heme prefers a nearly planar conformation in solution,<sup>7,11,13</sup> the question arises as to why such energetically unfavorable nonplanar conformations frequently occur in proteins, and what role if any they have in the function of the protein.

**Occurrence and Characterization of Nonplanar Heme Conformations in Proteins.** Nonplanar porphyrin macrocycles are observed in many heme proteins, although the largest distortions are seen in the *c*-type cytochromes and the peroxidases. Figure 1 shows the conformations of typical hemes in X-ray crystal structures of human hemoglobin and yeast mitochondrial cytochrome *c*.<sup>5</sup> In the linear displays of the heme shown in Figure 1, the *z*-displacements of the atoms relative to the mean plane of the macrocycle are expanded, to show more clearly the deviations from planarity. This type of display also clearly illustrates the variety and complexity of the heme distortions occurring in proteins.

Recently, we have devised a computational method which allows the nonplanar distortions to be quantified in terms of a few displacements along the most deformable normal coordinates of the  $D_{4h}$  symmetric porphyrin macrocycle.<sup>5,12</sup> This normal structural decomposition (NSD) procedure greatly simplifies the description of these geometrically complex structures. Furthermore, a simple bar graph of the displacements clearly shows the similarities and differences in the structures of the hemes. Figure 2 shows the NSD results for X-ray structures of a variety of types of proteins. The lengths of the bars represent the displacements along the lowest-frequency normal coordinates of each out-of-plane symmetry type that are required to give the best fit to the X-ray structure. Pure 1-Å displacements along each of these normal coordinates (normal deformations) are illustrated in Figure 3. These normal deformations form a (minimal) basis for characterizing the nonplanar distortions of the heme.<sup>5,12,16</sup>

The great variety in the types and magnitudes of the heme deformations in the proteins is clear from Figure 2. What is surprising is that in many cases these distortions are conserved for proteins of the same type that are obtained from different species. Figure 4 shows the NSD results for the hemes of three species for several different types of hemoproteins. Considering the approximately 0.1-Å errors in the atomic positions inherent in the X-ray crystal data, and thus in the deformations determined using NSD, the proteins within each type are remarkably similar. Individual displacements along the normal deformations of as large as 1.0 Å are observed.

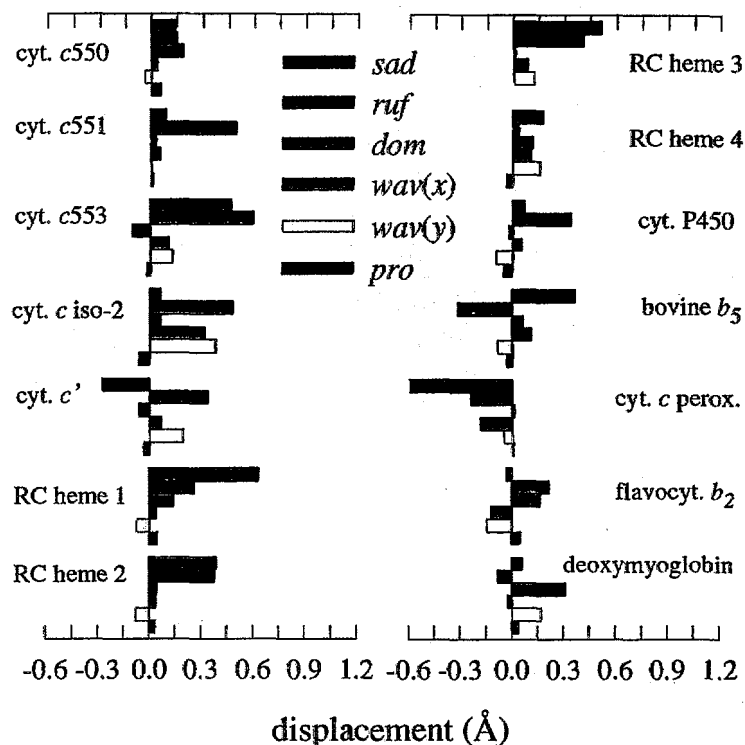


Figure 2. Normal structural decomposition results for X-ray crystal structures of a variety of types of hemoproteins.

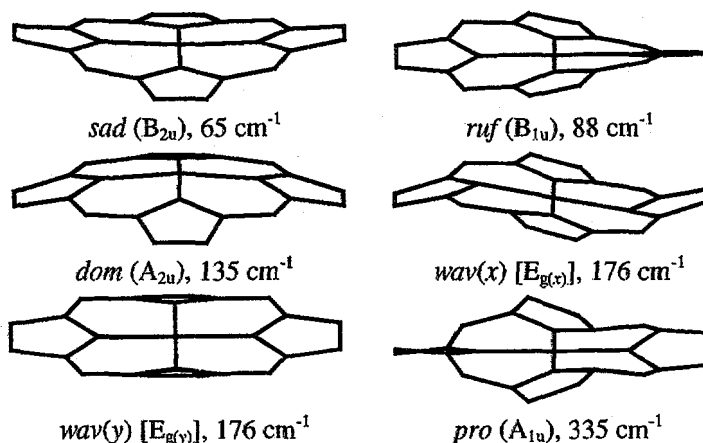


Figure 3. Symmetric normal deformations used to decompose the structures of hemes. (1-Å displacements are shown.)

It is clear from the NSD results that the heme conformation is conserved in many cases, and thus that it may play a role in the function of these enzymes. An alternative view is that the structure of the heme may just reflect the protein's tertiary structure, which is known to be remarkably similar for proteins within a class, and has little or nothing to do with function. Even in this case, the structure of the heme reflects the tertiary structure of the protein, and knowledge of the structure of the heme will provide a probe of the tertiary structure at the active site. Thus, it would still be useful to investigate the structures of the hemes in protein crystals and to develop spectroscopic means to determine their conformation in other environments.

*The Role of Nonplanar Conformers in Hemoprotein Function.* Several other developments suggest that a detailed investigation of the structural role of the heme in protein function is timely. First, a large number of studies of model nonplanar porphyrins has given new insight into the conformational flexibility of porphyrins and the energies and interactions necessary to produce nonplanar distortions.<sup>3,7,8,10,11,13-15,21-28</sup> More reliable spectroscopic probes of nonplanarity are a product of these investigations. In particular, resonance Raman spectroscopy has proved to be one of the best probes of the conformation of the porphyrin. In fact, it was the first technique to detect<sup>24</sup> and the only method currently known that can quantify the conformational equilibrium between planar and nonplanar forms of metal porphyrins.<sup>3,7,10a,24,25,28</sup> The high sensitivity and selectivity of resonance Raman spectroscopy are some of its well known advantages for exploring the structures of hemes.<sup>30</sup>

A second important recent development is that molecular modeling of porphyrins has reached new levels of accuracy in the prediction of porphyrin structures and conformational energies.<sup>7,8,11,13,15,16</sup> These new computational capabilities are essential because at present spectroscopic and crystallographic methods alone are inadequate for distinguishing and evaluating the types of distortions shown in Figure 3. Molecular mechanics calculations provide a useful tool for interpreting experimental results, and, when used judiciously, can be employed to differentiate between various scenarios in the absence of experimental data. Further, molecular mechanics calculations can predict the presence of conformers which may be energetically accessible, but not populated and thus not observed spectroscopically or in X-ray structures. Such stable conformational states of the heme may nevertheless have functional significance.

It is our goal to use these evolving new techniques in combination to investigate the role of protein-induced nonplanar distortions of hemes in the function of hemoproteins. The significance of the proposed work lies not

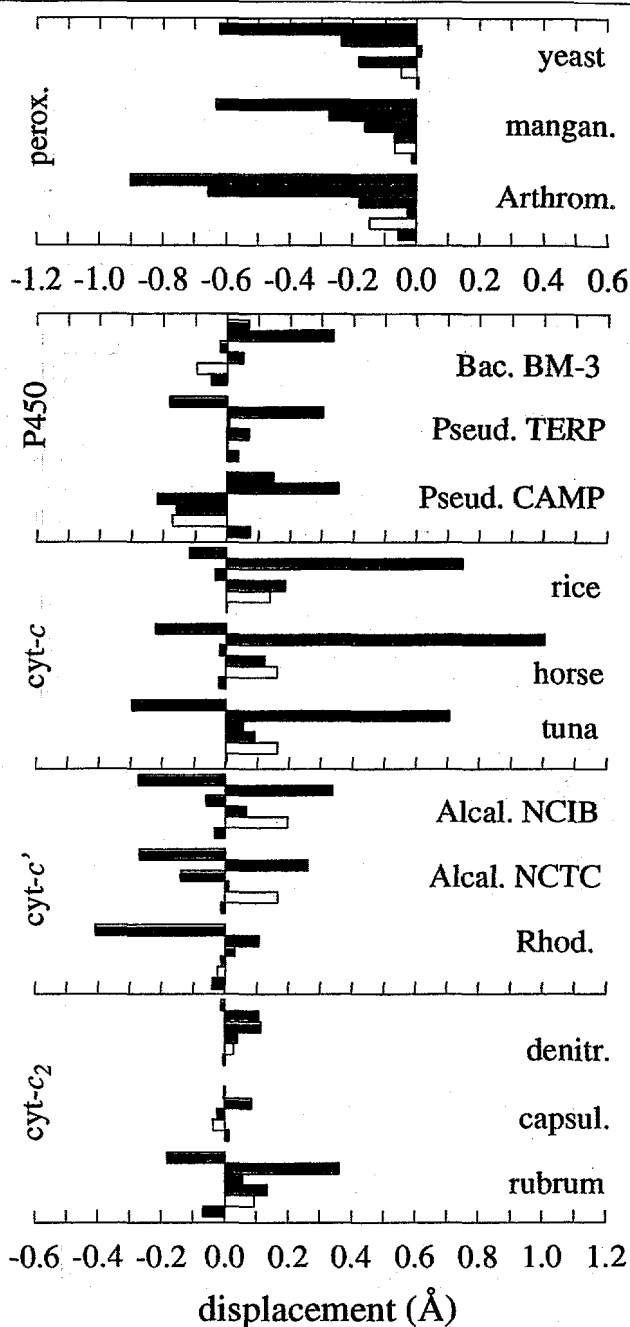


Figure 4. NSD results for 3 proteins from different species for several types of hemoproteins. For full details of the protein structures see reference 5.

only in an improved understanding of the fundamentals of hemoprotein function, but also in providing a fuller understanding of the relationship between the structure and function of metalloporphyrins in general. The proposed work should therefore aid in developing synthetic porphyrins for use in biomimetic processes and other commercial applications. This is another goal of the proposed research, one that is related to our efforts to use molecular design methods to tailor catalysts, sensor molecular-recognition elements, and optical materials.

*Protein Folding.* The protein-folding problem is to calculate the tertiary structure of a protein given its amino acid sequence. The ultimate goal is to fully understand how primary structure translates into three-dimensional structure and specific biological function of the protein. A secondary goal is to be able to design and produce synthetic proteins with tailored functionality. One problem with this scenario is that it is largely unknown how the protein conformation relates to function for many proteins. Given a functional role for nonplanar hemes, the hemoproteins offer a unique opportunity to investigate the consequences of protein folding on heme structure and function. Thus, another aim of the proposed work is to answer the question of how protein folding controls the heme distortion and its consequent reactivity. Molecular mechanics calculations and NSD of the heme conformation in proteins and in short heme-bound protein segments will reveal how the protein matrix controls the heme structure. In particular, the complex energetic landscape relating protein folding and heme conformation will be mapped out for heme-peptide fragments and hemoproteins like cytochrome *c*. Resonance Raman spectroscopy will be used to provide experimental validation of the results.

### c. Preliminary Studies / Progress Report

We start with a brief description of the normal structural decomposition method and its application to hemoprotein X-ray crystal structures. The NSD results for the *c*-type cytochromes will be shown to suggest a testable structural mechanism for the origin of the nonplanar distortion of the heme that is prevalent for most of the cytochromes *c*. As an illustrative example of the types of studies to be carried out, we will present preliminary data on nickel-reconstituted cytochrome *c* and its digestion product, nickel microperoxidase-11 (NiMP-11). The rationale for selecting this initial study will be given to illustrate how we expect other structural mechanisms to become evident from the NSD of the other hemoproteins, and how experimental systems will be chosen to validate the proposed mechanisms.

*Normal Structural Decomposition of the Out-of-Plane Distortions of Hemes of Proteins.* The NSD method is simple in concept.<sup>8</sup> It relies on the fact that the distortions of the 24 macrocycle atoms from ideal square-planar geometry can be given in terms of the  $3N-6 = 66$  normal coordinates of the macrocycle instead of simply giving the *x*, *y*, and *z* displacements of each atom in the porphyrin skeleton. The advantage of a description in terms of the normal coordinates is that the distortional energy of the macrocycle takes its simplest form in the normal mode representation. In particular, the distortion of the porphyrin takes place primarily along only the lowest-frequency normal coordinates because the restoring forces are smallest for displacements along these coordinates. In other words, the largest distortions are usually observed for the lowest-frequency normal coordinates because they are the softest modes of distortion.

A mathematical procedure has been described<sup>5,12</sup> which projects out the distortions from an ideal geometry (chosen to be a planar copper(II) porphine macrocycle) along the normal coordinates. The coordinate eigenvectors of each symmetry type are obtained from a normal coordinate calculation. Importantly, the lowest-frequency normal coordinate of each symmetry type is insensitive to the detailed nature of the metalloporphyrin force field. Figure 3 illustrates a 1-Å distortion along the lowest-frequency vibrational modes of each out-of-plane symmetry type that is used in our normal structural decompositions. One easily identifies each of these

normal deformations, *ruffling* ( $B_{1u}$ ), *saddling* ( $B_{2u}$ ), *doming* ( $A_{2u}$ ), *waving* ( $E_g$ ), and *propellering* ( $A_{1u}$ ), with various nonplanar conformations of the macrocycle that commonly occur in X-ray crystal structures of symmetrically substituted porphyrins.

For a given porphyrin structure, the computational procedure ascertains the contribution of each normal mode to that structure. For example, Figure 5 shows the X-ray crystal structure of nickel tetraphenylporphyrin along with the simulated structure obtained by adding up the projected-out displacements along only the *ruf*, *sad*, *dom*, *wav*, and *pro* normal coordinates.<sup>12,27</sup> Using only the displacements along these 6 lowest-frequency normal coordinates, addition of the individual displacements gives a simulated structure that closely matches the observed structure (orange dotted lines). In fact, for NiTPP only the *ruf* and *sad* deformations contribute to the distortion as shown in the histogram on the right in Figure 5.<sup>12,27</sup>

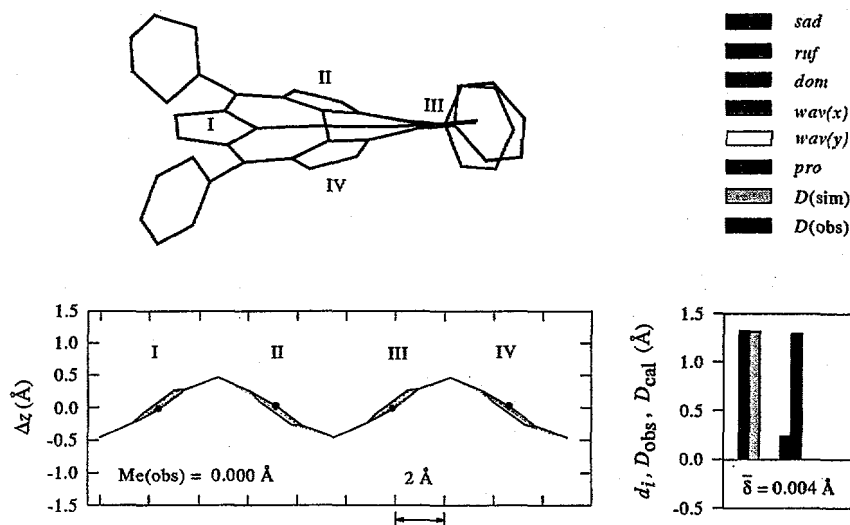


**Figure 5.** Linear display of the X-ray crystal structure of NiTPP (black) and the simulated structure (dotted orange) obtained by adding the displacements along the lowest-frequency normal coordinates of the out-of-plane symmetries. The bar graph gives the displacements along the out-of-plane normal coordinates that contribute to the linear combination comprising the simulated structure.

In general, an exact representation of the observed conformation usually requires that the deformations along additional normal coordinates be added into the simulated structure. However, an essentially exact representation of the structure always requires far fewer than the total number of out-of-plane normal coordinates ( $N-3 = 21$ ). On the other hand, when applied to protein crystal structures, the poorer resolution (compared to porphyrin crystals) usually precludes the determination of displacements for more than the lowest-frequency normal coordinates. That is, the high-frequency normal coordinate displacements are smaller than the statistical positional errors in the X-ray refinements. The dotted lines in Figure 1 show the simulated structures, based on just the lowest-frequency normal coordinates, for some hemes in protein X-ray structures. The deviations between the simulated and observed structures are addressed fully in a manuscript on NSD that is in press.<sup>5</sup>

**Structural Hypothesis for the Origin of the Nonplanar Distortion of the Heme of Cytochromes c.** Examination of Figure 1 shows that the most out-of-plane atom of the heme for yeast cytochrome *c* is the meso-carbon between pyrroles I and II. This is a general feature of the nonplanar conformations of the hemes of *c*-type cytochromes, and has led to the suggestion that the covalent attachments to the protein at the 2- and 4-positions of pyrroles I and II cause the distortion from planarity.<sup>6,20a</sup> Specifically, the short protein segment between the

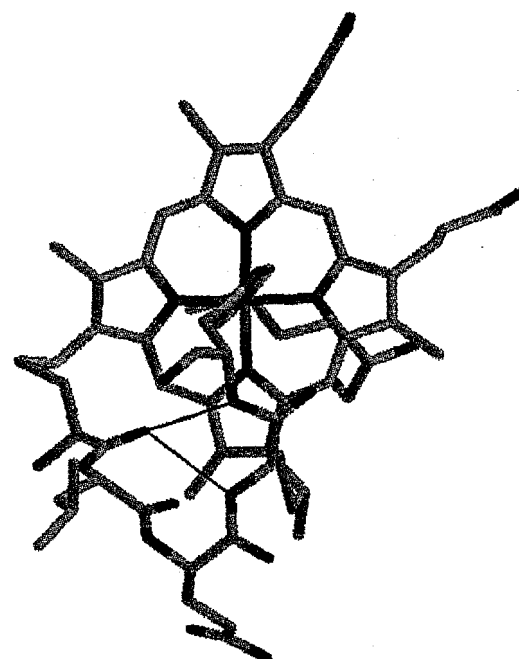


**Figure 6.** Hydrogen-bonding network in the peptide segment (CAQCH) of the horse cytochrome *c*, including the cysteines, the two residues between the cysteines, and the proximal histidine ligand of the iron atom.

cysteine residues could contract the distance between the thioether linkages to the heme, causing the porphyrin to buckle. In particular, we propose that the hydrogen-bonding network in this segment, illustrated in Figure 6, may act to contract this protein segment, giving rise to the nonplanar distortion.

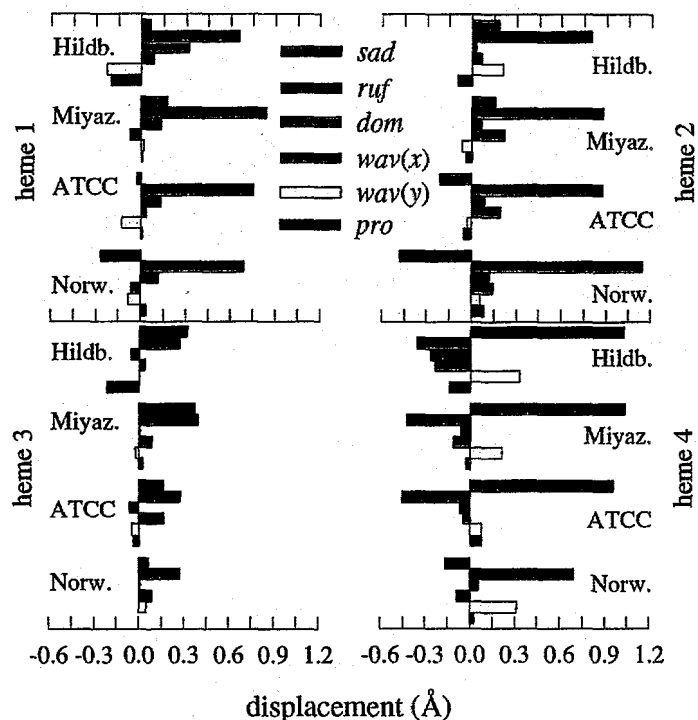


Figure 7. NSD results for the four hemes of cytochromes  $c_3$  isolated from different strains (Hildenborough and Miyazaki of *D. vulgaris* and ATCC and Norway A strains of *D. sulfuricans*).

Norway strains of *D. sulfuricans*. Also, notice that the predominant deformation becomes ruffling when only two residues intervene as for heme 1 of cytochromes  $c_3$  and the heme of the mitochondrial cytochromes  $c$ . Thus, these NSD results directly implicate the peptide segment between the cysteines in controlling the heme distortion.

The cytochromes  $c'$  provide another indication of the importance of the peptide segment that includes the cysteines and the proximal histidine, and further point to the importance of the hydrogen-bonding network in this peptide segment. Examination of the crystal structures of the cytochromes  $c'$  show that the conformation of this segment differs from that in the mitochondrial cytochromes  $c$ , resulting in only one hydrogen bond for the cytochromes  $c'$ . This difference in hydrogen bonding could account for the predominance of saddling in the cytochromes  $c'$  as opposed to ruffling for the cytochromes  $c$  (Figure 4).

In summary, it is clear from the NSD results for the  $c$ -type cytochromes that the peptide segment between the covalent cysteine linkages to the protein may be responsible for the distortion of the heme. Further, hydrogen bonding within the backbone of this segment may also be important in causing the distortion. We now give preliminary results obtained from experiments and calculations designed to test this structural hypothesis.

*UV-visible Absorption Experiments on Nickel-Reconstituted Cytochrome c and Nickel Microperoxidase-11.* The nickel derivatives were chosen for two reasons: first, a great deal of information on model nonplanar nickel porphyrins is available to aid in interpreting the spectral results reliably,<sup>1c,d,3,7-11,13-16,21-29</sup> and, second, the presence of nickel instead of iron insures that the proximal histidine will not be coordinated to the metal in the low and

Other support for this structural hypothesis comes from the NSD results for other cytochromes. The NSD results for the four-heme cytochromes  $c_3$ , given in Figure 7, are particularly convincing.<sup>5,12</sup> Hemes 2 and 4 typically have four intervening residues between the cysteines, whereas hemes 1 and 3 have two intervening residues as in the mitochondrial cytochromes  $c$ . Figure 7 shows that the heme conformations for these proteins are generally well conserved for different strains even though very little of the peptide is conserved. In fact, less than 10 residues (out of well over 100) other than the cysteines and histidines bound directly to the hemes are conserved for the strains listed. The maintenance of the structure of the heme with so little sequence homology between the strains suggests that only a small portion of the protein is required to generate the major part of the distortion.

A striking difference in conformation is noted (Figure 7) for the Norway strain for heme 4 compared to hemes 4 of the other strains; this conformational difference most likely results from the deletion of two of the four residues between the cysteines for the

high pH regions of the protein and at all pH values for NiMP-11 (*vide infra*). Both of these consequences of nickel replacement help to simplify the interpretation of the spectroscopic results. Additional advantages of nickel reconstitution will become clear in the discussion that follows.

**Nickel Microperoxidase-11.** In a Raman study of iron(III) MP-8 by Desbois and coworkers,<sup>28</sup> they showed that the nonplanar conformers observed in the X-ray structures of Cyt-c are probably also present in MP-8 in aqueous micellar solution, and that the nonplanar conformation is essentially due to the three-point attachments between the heme and protein, *i.e.*, the two thioether bridges and the Fe-His bond. Indeed, replacement of the proximal His with an exogenous His ligand results in a less distorted heme, based on the shifts in the frequencies of two distortion-sensitive Raman lines,  $\nu_8$  and  $\nu_{10}$ . The use of these lines as markers for porphyrin nonplanarity is based on the known behavior of these lines upon ruffling of nickel porphyrins, which is due primarily to the work of our group.<sup>3,8,24,25</sup> The detailed pH dependence of the distortion was not addressed in this work.

Replacement of Fe with Ni lowers the affinity of the metal for His as an axial ligand, effectively breaking the metal-His bond for NiMP-11 at the pH extremes. Thus, based on the results of Desbois and coworkers,<sup>28</sup> we would then expect the Ni porphyrin of MP-11 and Cyt-c to be less distorted than the iron derivatives because of the missing metal-His bond; on the other hand, the small Ni(II) ion favors certain types of nonplanar distortions.<sup>16</sup> Nonetheless, the absence of axial coordination and presence of well-characterized Ni as the central metal allows an unambiguous interpretation of the data for NiMP-11 (and the four-coordinate forms of NiCyt-c). The pH-dependent absorption spectra that have been obtained (not shown) allow the influence of the hydrogen-bonding network in the Cys-X-Y-Cys-His segment to be investigated without the interference from most of the rest of the protein. In particular, the spectra show that NiMP-11 is predominantly four-coordinate over the entire pH range from 0.2 to 13.0.

**Nickel Cytochrome *c*.** Absorption spectra of NiCyt-*c* were obtained in the pH range from 0.5 to 14.0. The absorption spectra of NiCyt-*c* are shown in Figure 8 for the pH range from 0.5 to 7.0. By comparison with spectra of model Ni porphyrins, the major changes in the spectrum can be ascribed to loss of the histidine ligand at low pH ( $pK_a$  3.5), although more subtle changes in the spectrum are also evident. At present, we cannot say with certainty whether the methionine ligand is bound near neutral pH or not; however, the blue shift of the Soret-band maximum relative to six-coordinate models suggests that the methionine may not be bound. Further work will address this question.

At least two additional forms are evident in the spectra in the pH region from 0.5 to 3.0 in the top panel of Figure 8 based on the lack of isobestic points. These forms are four coordinate and probably differ in the conformation of the Ni porphyrin.

Spectroscopic studies of ferricytochrome *c* by others<sup>31</sup> have demonstrated the presence of at least four conformational states of the native iron protein in this pH region. The conversions between the protein conformational states  $III_s \leftrightarrow III_{s,a} \leftrightarrow II_s \leftrightarrow I_s$  occur with  $pK_a$ 's of 3.5, 2.2 and 1.1. The state  $III_{s,a}$  is folded in about the same way as  $III_s$  but the heme crevice is loosened. Also the spin state and coordination configuration

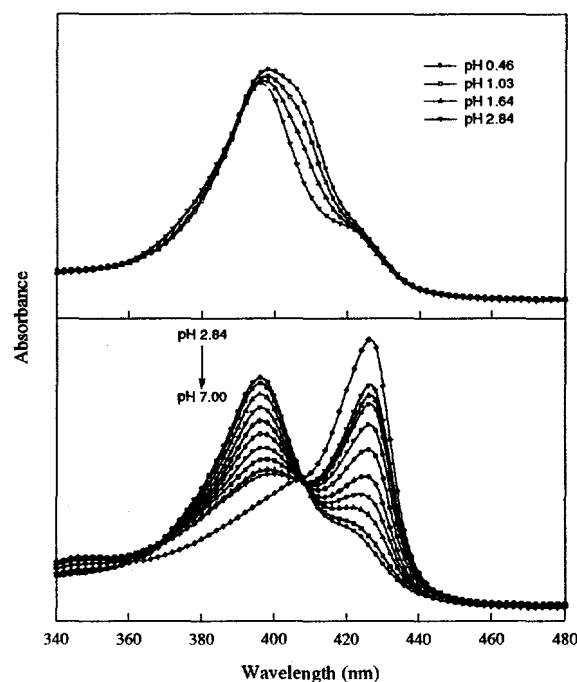


Figure 8. Soret band region of the absorption spectrum of Ni cytochrome *c* at different pH values.

is similar to that of III<sub>s</sub>. The two protein forms below pH 3 are essentially folded forms, but with a smaller degree of protein secondary structure and altered axial coordination. State II<sub>s</sub> has high-spin six-coordinate heme with His and a water molecule as ligands. State I<sub>s</sub> is five-coordinate with His as the only ligand.

Similar protein conformational states appear in NiCyt-c. The pK<sub>a</sub> of the His or His/Met ligand loss occurs at about pH 3.5, the pK of the loosening of the heme crevice in ferricytochrome. See Figure 9. It was thought that the disruption of the secondary structure in the low-pH conformational states of the iron protein, states II<sub>s</sub> and I<sub>s</sub>, might also happen in the nickel protein below pH 3. This might weaken the hydrogen bonding within the peptide segment that includes the cysteines and thus decrease the degree of nonplanarity of the porphyrin macrocycle. Indeed, changes in the structure of the four-coordinate Ni porphyrin of NiCyt-c are evident in the Soret-band spectral changes in the pH region from 0.5 to 2.8 (Figures 8 and 9). These changes suggest that similar protein conformational states exist regardless of the metal. The absorption spectrum changes can be ascribed to increased occupation of a planar form as the pH is lowered on the basis of the resonance Raman spectra (*vide infra*). However, it should be noted that nonplanar forms are usually associated with a red shift in the Soret relative to the planar form, not a blue shift as seen in the spectra of Figure 8.

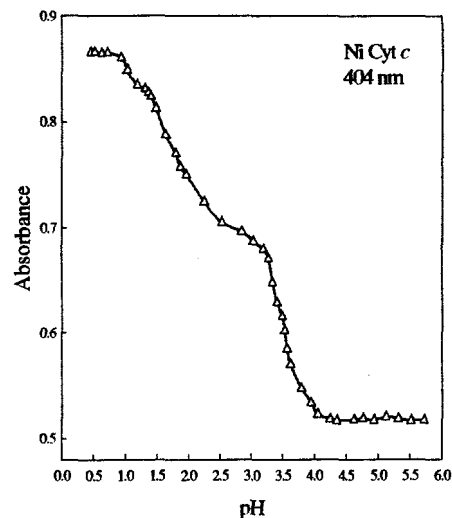


Figure 9. Absorbance at 404 nm as a function of pH at constant chloride concentration.

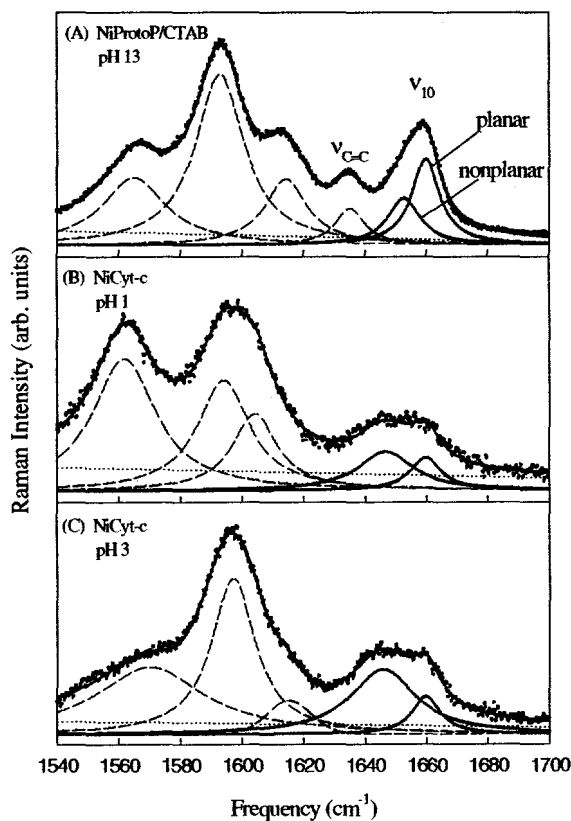


Figure 10. Resonance Raman Spectra of Nickel Cytochrome *c* (B and C) and four-coordinate NiProtoP in CTAB (A).

Even if the protein does show a less distorted porphyrin at very low pH consistent with our hypothesis, we cannot conclude that a particular peptide segment actually causes the heme distortion based on the NiCyt-c results alone. The problem is that we cannot say what part of the protein is important; we only know that the weakening of the secondary structure may be important. For this purpose, a study of Ni microperoxidase-11 was initiated. MP-11 has an attached eleven amino-acid segment that includes the 5-residue CAQCH segment of interest. The pH-dependent absorption and resonance Raman spectra of NiMP-11 in the presence and absence of detergent were obtained. The presence of cetyltrimethylammonium bromide (CTAB) above the CMC was used to prevent aggregation of NiMP-11. NiMP-11 has the additional advantage of being mostly four-coordinate at all pH's, making interpretation of the data in terms of macrocyclic distortions uncomplicated by axial coordination changes.

*Resonance Raman Spectra of Nickel Cytochrome c and Nickel Microperoxidase-11.* Nickel Cytochrome *c*. Figure 10 shows the resonance Raman spectra of NiProtoP in aqueous CTAB solution and the spectra of NiCyt-c at pH 1 and 3 obtained with 413.1-nm excitation. The spectral region shown contains the Raman line  $\nu_{10}$  that is most sensitive to nonplanar distortion of the porphyrin because of the large downshifts that occur. Also, the region of the spectrum near  $\nu_{10}$  is not

complicated by spectral crowding as is the rest of the spectral region shown in Figure 10. Anticipating the presence of multiple forms and noticing the broadness of  $\nu_{10}$ , we have resolved  $\nu_{10}$  into two sublines as shown (solid lines). The high-frequency subline in each case is associated with the planar form based on its frequency ( $1660\text{ cm}^{-1}$ ); the low-frequency sublines are associated with nonplanar forms. (These assignments are based on single-crystal Raman spectra for which the macrocycle has a known conformation.) Even ignoring the possibility of resonance excitation effects which favor the nonplanar form, the planar form clearly dominates for the NiProtoP model compound. Similar ratios of nonplanar-to-planar intensities are observed for other nickel-porphyrin models, including Ni octaethylporphyrin (NiOEP)<sup>3,7,22,24,25</sup> and Ni tetraphenylporphyrin (NiTPP).<sup>27</sup> We have also shown that Ni mesoporphyrin (NiMesoP) shows a similar ratio of nonplanar-to-planar intensities, so the presence of the vinyl groups of NiProtoP does not affect the ratio to a significant extent.

Most interesting is that the relative intensity of the nonplanar subline is much greater for NiCyt-c at both pH values than for the NiProtoP model. The ratio of intensities (nonplanar/planar) is 0.6 for NiProtoP, 2.1 for NiCyt-c at pH 1, and 3.8 at pH 3. Thus, it appears that the macrocycle is becoming more distorted as the secondary structure, including the H-bonding in the peptide backbone, becomes more established around pH 3. Also, the nonplanar conformers of NiCyt-c are considerably more nonplanar than for the model compound, based on the lower frequencies of the sublines for NiCyt-c ( $1647\text{ cm}^{-1}$  at pH 1,  $1646\text{ cm}^{-1}$  at pH 3) compared to NiProtoP ( $1653\text{ cm}^{-1}$ ). Further, the degree of distortion of the macrocycle becomes somewhat greater at the higher pH, as expected when the H-bonding network is established within the secondary structure of the protein. Thus, the Raman data for NiCyt-c are consistent with the hypothesis that H-bonding in the heme-linked pentapeptide is responsible for the macrocyclic distortion, but does not rule another part of the protein as its origin.

Nickel Microperoxidase-11. The resonance Raman data for NiMP-11 shows more conclusively that the specified pentapeptide is involved since little of the protein besides this pentapeptide remains. Figure 11 shows the Raman spectra of NiMP-11 under various solution conditions. In CTAB, where aggregation of MP-11 is not a problem, the Raman spectrum of NiMP-11 at pH 13 is very similar to that of NiCyt-c. Decomposition of  $\nu_{10}$  into two sublines gives an intensity ratio of 2.9 and frequencies similar to those of NiCyt-c for both the planar and the nonplanar conformers. The frequency of the nonplanar form is slightly higher than that for NiCyt-c at pH 1 and 3. Thus at pH 13 in CTAB, the presence of the peptide segment shifts the equilibrium heavily in favor of the nonplanar form, just as does the entire protein component in the case of NiCyt-c. Our preliminary Raman results show that the ruffling of NiMP-11 increases with pH up to 13 in CTAB solutions. In aqueous solutions of NiMP-11, the relative intensities of the planar and ruffled sublines hardly changes at all in the pH range from 1 to 13. We believe the hydrophobic environment required for a strong H-bond network to form and exert its force on the macrocycle is not established in CTAB until the heme-peptide becomes sufficiently negatively charged somewhere above pH 10. Further, experiments are required to determine the exact pH at which the ruffling of NiMP-11 occurs and the specific cause of the nonplanar distortion.

In summary, both the absorption and Raman data for NiCyt-c and NiMP-11 are fully consistent with the proposed structural mechanism of heme distortion for the cytochromes. The spectra are also consistent with previous studies of FeCyt-c and FeMP-8, including variable pH protein-folding studies.<sup>28,31</sup>

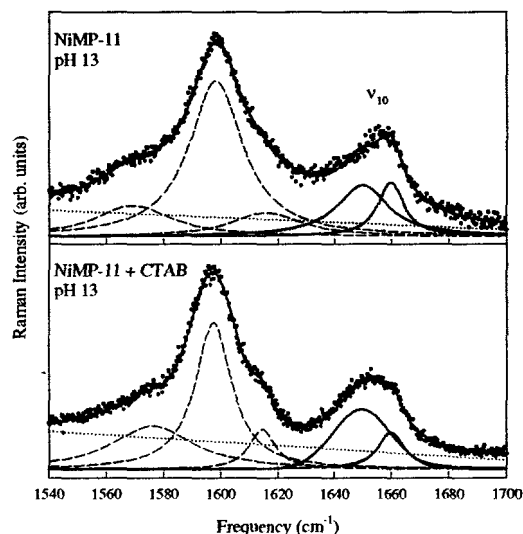


**Figure 11.** Resonance Raman Spectrum of nickel microperoxidase-11 in the presence and absence of CTAB showing the curve fitting analysis.

**FeMP-5 Molecular Mechanics Calculations.** Molecular mechanics calculations can greatly aid in locating the site(s) in the protein that produces the nonplanar distortion of the heme. For the cytochromes *c*, we can calculate the structure of the heme with various attached protein components to test the hypothesis that the distortion is caused by the pentapeptide. Figure 12 shows the calculated structures of pentapeptide-bound heme as well as several model Fe(III) porphyrins. The calculations show that the pentapeptide alone can account for the degree of ruffling of the heme found in the crystal structures of cytochromes *c*.<sup>6</sup>

Panel A of Figure 12 shows the energy-optimized structure of Fe(III) protoporphyrin IX (FeProtoP), which is almost planar (average pyrrole ruffling dihedral angle is less than 1°). Panel B shows the effect of thioether modifications of the vinyl substituents of FeProtoP. The ruffling is probably exaggerated because the calculation done in vacuum, possibly favoring agglomeration of the bulky substituents more than would occur in solution. Panel C shows the effect on the ruffling of the CAQCH pentapeptide unit, but without the His-Fe bond being present. And, finally, Panel D shows the effect of the pentapeptide unit when all three attachments to the protein are intact. In the latter case, the angle is 14°, the same as the average ruffling angle for all of the available X-ray structures of the mitochondrial cytochromes *c*. Addition of more amino acids to either end of the pentapeptide unit has little further influence on the heme structure.

The three-point connection of the pentapeptide is sufficient, in fact, to explain most of the normal deformations making up the observed distortion of the heme of the cytochromes *c*. Specifically, the *ruf* and *x*- and *y-wav* contributions are qualitatively predicted by the calculated structures of FeMP-11 for the horse and tuna proteins as can be seen in Figure 13. However, the negative *sad* deformation is not reproduced by the calculated FeMP-11 structures. The *sad* deformation probably arises from additional heme interactions with the protein (e.g., H-bonding to the propionates) or else from a difference in the conformation of the pentapeptide segment due to its interaction with the rest of the protein component. (Also, see the discussion of the natural variation in X of the Cys-X-Y-Cys-His segment in the next section.)

**Porphyrin Structural Characterization Methods.** The above discussion of our preliminary results aimed at elucidating the structural mechanism of heme distortion in the mitochondrial cytochromes *c* illustrates the methods that will be used in the proposed studies of the cytochromes and other hemoproteins. The combination of theoretical and experimental techniques, including molecular mechanics calculations, normal structural decompositions, and spectroscopic methods is a crucial viewpoint for approaching this problem. The recent development of the NSD method gives us a particularly important new tool for successful completion of our research goals. The molecular modeling methods and the NSD methods will be described more fully in the Research Design and Method section.

Another advantage is our extensive experience with model nonplanar porphyrins and our contribution to the

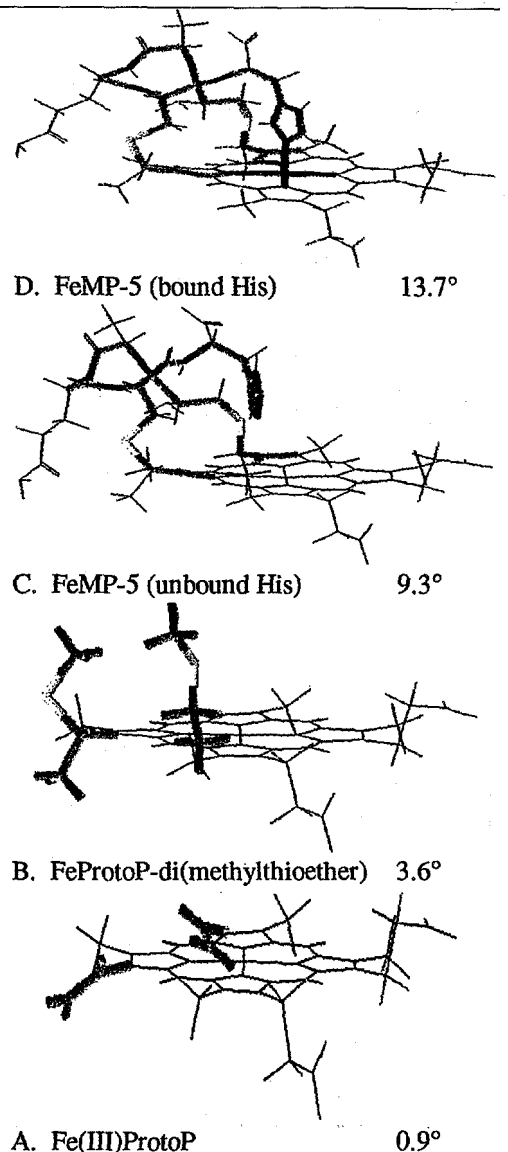
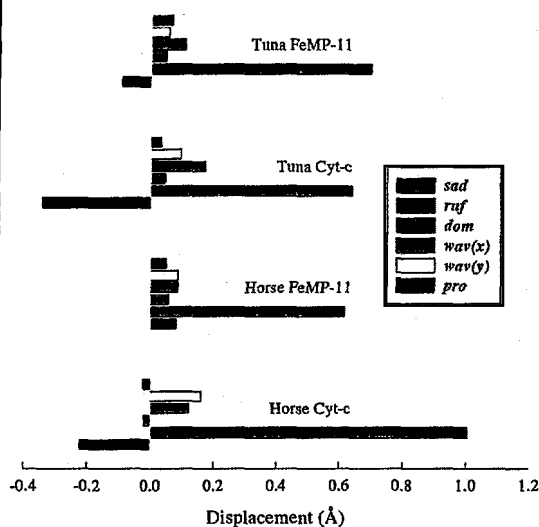


Figure 12. Effects of various 2- and 4-substituents and interactions on the CaN-NCa ruffling dihedral angle of opposite pyrrole planes.

Cys-X-Y-Cys-His segment in the next

development of resonance Raman spectroscopy as a means of quantifying the type and magnitude of distortion.<sup>7,8,10,11,13,14-16,21-24,26,27</sup> We now outline major conclusions of our recent studies of model nonplanar porphyrins, in the context of the work of others, to demonstrate the level of understanding attained and to provide the background for a discussion of the proposed new research in this area.



**Figure 13.** NSD results for calculated structures of FeMP-11 from horse and tuna and the observed structures of the corresponding cytochromes c.

proximal His. This was a particularly interesting finding in that the protein was shown to exercise direct control over the macrocycle structure through only nonbonding interactions. Subsequent to these findings in 1989 and 1990, we began a series of investigations<sup>8,9</sup> of nonplanar synthetic porphyrins in collaboration with Prof. Kevin Smith and, at the same time, we began a Raman investigation of the structure of cofactor F430 of methylreductase.<sup>10</sup> F430 is a Ni corphin which facilitates methylreductase activity. Reduction of the porphyrin ring in F430 facilitates changes in the oxidation state of the Ni atom by increasing the out-of-plane flexibility of the macrocycle.<sup>29</sup> The Raman studies of the model compounds provided a correlation between the frequencies of the structure-sensitive marker lines and the degree of nonplanarity of the macrocycle.<sup>8,9</sup>

As the prevalence of nonplanar porphyrin conformers and their possible importance in biological systems became evident, our studies became more diverse including a wider range of nonplanar porphyrin models and other spectroscopic probes, primarily NMR and X-ray crystallography.<sup>15,26</sup> These studies verified the structure-frequency relationships for a broader range of porphyrins and also served to refine and validate the predictions of our molecular mechanics force field (*vide infra*). They also elucidated the important role of the substituents and their orientations in determining the nonplanar conformation, the effect of the nonplanar conformation on axial ligand orientation, the existence of nonplanar conformational isomers at higher energy than the ground-state conformer, ring current effects, and macrocycle inversion processes. In some cases a number of stable conformers (local minima) are thermally occupied at room temperature.<sup>14,15c,g</sup> These thermally accessible conformers may play a role in some biological processes.

Other investigations of nonplanar porphyrins looked at the effect of the central metal on nonplanar structure using resonance Raman spectroscopy.<sup>7,11,13</sup> These studies also served to develop suitable force-field parameters for Co, Cu, Zn, Pd, and Fe for the molecular mechanics calculations. The results show that large metals reduce the magnitude of the distortion for highly sterically crowded porphyrins. The metal size was also found to reduce the slope of the well-known core-size correlations for the structure-sensitive Raman lines. For porphyrins that coexist in both planar and nonplanar conformers, increasing the metal size shifts the equilibrium in favor of

the planar form.<sup>13</sup> The latter work also provides an estimate of the steric repulsion energy necessary to cause the distortion. The study also showed that Fe porphyrins should exhibit only the planar conformer for biological porphyrins like FeProtoP in the absence of a perturbing protein environment.

Different types of deformations were examined in recent investigations.<sup>8,16</sup> A series of nickel *meso*-tetraalkyl-substituted porphyrins with alkyl groups of varying steric size exhibit nearly pure *ruf* deformations.<sup>8</sup> The magnitude of the distortion increases with the bulkiness of the substituent, so the variation of the Raman-line frequencies and absorption-band positions were determined and correlated with molecular mechanics structural parameters and transition energies calculated using INDO/s semiempirical methods. A study of 5,15-dialkyl substituted porphyrins investigated the consequences of the addition of a *dom* deformation to the *ruf* deformation.<sup>16</sup> Differing dependencies of the Raman frequencies on the magnitude of the distortion were found when the *dom* and *ruf* deformations are both present in the structures. This work also represents the first use of the NSD method for analyzing porphyrin structures, and in this case both calculated and X-ray structures were available for comparison.

Because almost all Ni porphyrins show ruffled conformers, we became interested in whether Ni porphine (NiP) with only hydrogen substituents would also be nonplanar.<sup>21</sup> That is, whether at least some steric interaction of the peripheral substituents is necessary to observe nonplanar conformers. An X-ray crystal structure of NiP was obtained. Together with the Raman spectra taken both in solution and in the crystal, the data show that NiP exists in solution only as the planar species.<sup>21</sup>

*Structure-Reactivity Relationships in Model Porphyrins.* Functional properties of tetrapyrroles that are affected by nonplanar distortion include absorption-band energies and extinction coefficients (e.g., Figures 8 and 14) and other photophysical properties like excited state lifetimes.<sup>33</sup> Studies by our group and others have shown that nonplanar distortions influence the oxidation potential of the porphyrin ring.<sup>34,35</sup> Macrocycle distortion may also influence metal oxidation and reduction potentials.

Ligand binding chemistry is another property that is influenced dramatically by nonplanarity of the porphyrin macrocycle. Figure 14 shows the absorption spectra of a series Ni derivatives of *meso*-tetraalkylporphyrins (the alkyl groups are Et = ethyl, Pr = propyl, Pe = pentyl, Me = methyl, iPr = isopropyl, cH = cyclohexyl, and tBu = tert-butyl.) in neat piperidine solution. In this coordinating solvent, planar NiTPP (Ph = phenyl) is almost fully six-coordinate. The alkyl porphyrins, in contrast, are only partially six coordinate.

The four-coordinate Soret-band peak positions are indicated by the blue line and the six-coordinate peaks are indicated in red. The red shift in the Soret band of the four-coordinate species resulting from increasing nonplanar distortion is evident. The six-coordinate Soret bands are at almost identical wavelengths because the large high spin Ni ion causes the macrocycle to be nearly planar for the porphyrins for which a six-coordinate species is observed. The amount of the six-coordinate species, obtained from the relative areas of the two Soret bands, decreases as the substituents become larger, with no six-coordinate form at all observed for the secondary

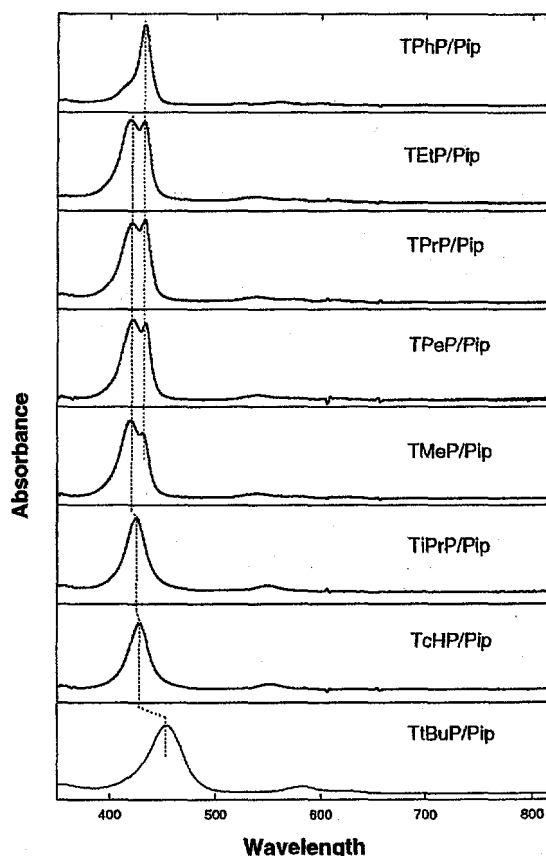


Figure 14. Absorption spectra of a series of *meso*-tetra-alkyl-substituted porphyrins with progressively more bulky alkyl groups (top to bottom).

and tertiary alkyl substituents. The equilibrium constants in pyrrolidine,  $K_1K_2$ , are 25 for NiTPP, 0.50 for NiTPrP, 0.34 for NiTPeP, and 0.18 for NiTMeP. The observed decreasing axial ligand affinity with increasing nonplanarity cannot be explained by electron-donation effects of the substituents since the alkyl substituents differ only marginally in this respect. The preliminary evidence indicates that the equilibrium constant  $K_1$  for addition of the first ligand is much larger than  $K_2$  for addition of the second ligand when the porphyrin is nonplanar. This probably occurs because energy is required to make the nonplanar macrocycle go planar in order to accommodate the larger high-spin nickel atom, thus lowering the binding energy for the first ligand. Since the spin-state-change and the core-expansion energies are expended on addition of the first ligand, the second axial ligand binds much more easily. Further studies are underway to define the relationship between axial ligand reactivity and nonplanar distortion.

#### d. Research Design and Methods

*Normal Structural Decomposition of Heme Protein Crystal Structures.* Our first task will be to structurally decompose the greater than 500 hemes contained in all 325 hemoprotein crystal structures in the Brookhaven protein data bank (PDB). The NSD results will be published as parts of papers on various aspects of the structural motifs discovered and also made available to other researchers on the Internet. Several possible structural motifs have already been noticed for subsets of the proteins and these will be the initial targets of the complete NSD analysis of the PDB structures. Some examples of possible structural motifs of the heme that have been recognized so far are:

(1) It has been suggested that oxidation state and spin state of the iron influence the metal size and thus the tendency of the porphyrin to undergo certain distortions.<sup>20a,36</sup> For the cytochromes *c*, this tendency, if present, is probably not statistically significant in the presently available NSD data. We will consider this hypothesis using NSD in all of the hemoproteins, classified according to oxidation and spin states of the iron, to see if this proposal is born out in the complete body of crystallographic data.

(2) Axial coordination of exogenous ligands influences the electronic properties of the iron, its location relative to the macrocycle, and may also influence biological activity. On the other hand, our preliminary analysis of current NSD results suggests that axial ligation may have less effect on the structure of the macrocycle than one might expect. We intend to determine the influence of axial ligation on the macrocyclic structure by using NSD to examine all proteins for which structures are known for both the unbound protein and the protein with bound exogenous ligands. This will also reveal the effect of different ligands on the distortion of the porphyrin macrocycle.

(3) Experimental and theoretical studies have suggested that orientations of the endogenous axial ligands influence the out-of-plane distortion of the macrocycle, and that the converse is also true.<sup>15e,37</sup> We will determine how axial ligand orientation correlates with heme structure in the hemoproteins. Preliminary indications are that ligand orientation may influence the macrocyclic structure in the proteins but that it is not the determining factor. In addition, the macrocycle distortion can have a strong influence on ligand orientation. However, many examples can be found in the protein crystal data that suggest that out-of-plane distortion alone does not control the ligand orientation. Addressing these questions in the complete body of X-ray crystal data by NSD analysis will lead to a greatly increased understanding of the role of axial ligation in determining macrocycle structure, and vice versa.

Of course, we will identify all protein types for which the heme conformation is conserved. In the course of

these NSD studies, the detailed X-ray structure of each protein will be examined to try to determine the structural origin of the heme distortion. To date, we have mainly concerned ourselves with similarities between heme structures in proteins of the same type, whereas closer examination of the differences between structures in related proteins may reveal the influence of the amino acid sequence on heme conformation. These NSD analyses will be performed at UNM by the PI, postdocs and graduated students.

*Normal Structural Decomposition of Synthetic Porphyrin Crystal Structures.* We will structurally analyze most if not all of the roughly 1300 crystal structures of porphyrins in the Cambridge structural data bank. Preliminary analysis of some of these structures indicates a wealth of information on the causes of nonplanar distortions of porphyrins. For example, the NSD data so far examined indicate that crystal packing forces influence macrocycle structure primarily by determining peripheral substituent orientations. The fixed substituent orientations then account for the macrocycle conformation. This and other hypotheses will be investigated. Finally, NSD analysis of crystal structures of synthetic porphyrins will also give information on the contribution of other deformations besides the lowest-frequency ones. This structural information is not obtainable from NSD studies of the protein crystals because of the inherently larger uncertainties in the atomic positions. This work will be done by personnel at UNM.

*The Normal Structural Decomposition Method: A Minimal Basis for the Description of Nonplanar Heme Distortions.* We now provide a brief description of the NSD method. The description of the nonplanar distortion of a porphyrin in terms of equivalent displacements along the out-of-plane normal coordinates provides a uniquely useful framework for analyzing porphyrin structures. The lowest-frequency normal coordinates of each symmetry type are the softest modes of distortion, *i.e.*, the restoring forces (or macrocyclic distortion energies) are the smallest for displacements along these normal coordinates. Thus, these deformations are expected to predominate in the observed heme distortion. Further, because the out-of-plane displacements along these normal coordinates are the largest, they are the most statistically significant in the reported heme decomposition results. Expressing the distortion in terms of only the six (out-of-plane) normal deformations [*sad* ( $B_{2u}$ ), *ruf* ( $B_{1u}$ ), *dom* ( $A_{2u}$ ), *wav*( $x$ ), *wav*( $y$ ) ( $E_g$ ), *pro* ( $A_{1u}$ )] also yields a much simpler description of the heme conformation.

The static 1-Å deformations along the lowest-frequency out-of-plane normal modes of each symmetry type form a minimal basis for describing the distortions. In fact, only five values must be given to characterize the heme structures in the protein because the *pro* deformation is usually too small to be statistically significant (*vide infra*). For these reasons, only a simplified version<sup>5</sup> of the full procedure for normal structural decomposition<sup>12</sup> is herein described and is sufficient for analysis of the hemoprotein crystal structures.

*Linear Combinations of the Minimal-Basis Normal Deformations.* Figure 3 illustrates the static 1-Å deformation along the lowest-frequency normal mode of each out-of-plane symmetry type. The atomic displacements shown and the frequencies given in Figure 3 are for the normal modes of the  $D_{4h}$ -symmetric copper macrocycle that is used as a reference structure. (A complete discussion on the choice of this reference structure is given in reference 12.) Briefly, the energy-minimized reference structure and its normal modes are calculated using a molecular mechanics force field developed for metalloporphyrins and the VIBRATE routine of POLYGRAF (Molecular Simulations).<sup>8,11,16</sup> The normalized static displacements shown in Figure 3 are defined in non-mass-weighted coordinate space and are referred to as normal deformations. An observed structure is analyzed by projecting out the optimum displacement along these normal deformations [*sad*, 65  $\text{cm}^{-1}$ ), (*ruf*, 88  $\text{cm}^{-1}$ ), (*dom*, 135  $\text{cm}^{-1}$ ), [*wav*( $x$ ), *wav*( $y$ ), 176  $\text{cm}^{-1}$ ], and (*pro*, 335  $\text{cm}^{-1}$ )].<sup>5,12</sup> A simulated heme structure is obtained by forming the linear combination of normal deformations determined by these displacements. Then the simulated and observed structures are compared in a linear display as shown in Figures 1 and 5.

Mathematically, the nonplanar heme distortion is simulated by the optimal linear combination of the six normal deformations according to:

$$\Delta \mathbf{z}_{\text{sim}} = d_{\text{sad}} \hat{\mathbf{D}}_{\text{sad}} + d_{\text{ruf}} \hat{\mathbf{D}}_{\text{ruf}} + d_{\text{dom}} \hat{\mathbf{D}}_{\text{dom}} + d_{\text{wav}(x)} \hat{\mathbf{D}}_{\text{wav}(x)} + d_{\text{wav}(y)} \hat{\mathbf{D}}_{\text{wav}(y)} + d_{\text{pro}} \hat{\mathbf{D}}_{\text{pro}} = \sum_{k=1}^6 d_k \hat{\mathbf{D}}_k, \quad (1)$$

where  $\Delta \mathbf{z}_{\text{sim}}$  is the 24-dimensional vector of displacements of the macrocyclic atoms from the mean plane in the simulated structure. The normalized vectors  $\hat{\mathbf{D}}_k$  are the 24-dimensional basis vectors (normal deformations) shown in Figure 3; the subscript  $k$  designates the *sad*, *ruf*, *dom*, *wav(x)*, *wav(y)*, and *pro* normal-deformation types. The atomic displacements for each normal deformation are given in the Supporting Information of reference 12. The scalar coefficients  $d_k$  (in Å) are the displacements along the normal deformations  $\hat{\mathbf{D}}_k$ .

*Determination of the Displacements along the Normal Deformations.* The displacements  $d_k$  in Eqn. (1) are obtained by the least-squares method. That is, the values of  $d_k$  are determined by requiring that the sum of the least-squares residuals between the simulated,  $\Delta \mathbf{z}_{\text{sim}}$ , and observed,  $\Delta \mathbf{z}_{\text{obs}}$ , distortions be a minimum,

$$f(d_k) = |\Delta \mathbf{z}_{\text{sim}} - \Delta \mathbf{z}_{\text{obs}}|^2 = \left| \sum_{k=1}^6 d_k \hat{\mathbf{D}}_k - \Delta \mathbf{z}_{\text{obs}} \right|^2 \stackrel{!}{=} \text{minimum}, \quad (2)$$

where the vertical bars represents the norm of the vector. Eqn. (2) requires six equations,

$$\frac{\partial f(d_k)}{\partial d_k} = 0, \quad \text{where } k : \text{sad, ruf, dom, wav}(x), \text{wav}(y) \text{ and } \text{pro}. \quad (3)$$

Since the normal deformations are orthogonal by symmetry ( $\hat{\mathbf{D}}_k' \hat{\mathbf{D}}_j = \delta_{kj}$ ), the solution is simply given by the vector product,

$$d_k = \hat{\mathbf{D}}_k' \Delta \mathbf{z}_{\text{obs}}. \quad (4)$$

The set of displacements  $d_k$  determines the *total* simulated distortion  $D_{\text{sim}}^{\text{oop}}$  (in Å). Using Eqn. (1), we then obtain,

$$D_{\text{sim}}^{\text{oop}} = |\Delta \mathbf{z}_{\text{sim}}(d_k)| = \sqrt{\sum_{k=1}^6 d_k^2}. \quad (5)$$

The total observed distortion  $D_{\text{obs}}^{\text{oop}}$  is given by the observed atomic  $\Delta z$  displacements of each of the 24 macrocyclic atoms  $(\Delta z_n)_{\text{obs}}$  with respect to the mean plane,<sup>5,12</sup>

$$D_{\text{obs}} = \sqrt{\sum_{n=1}^{24} (\Delta z_n)_{\text{obs}}^2} = |\Delta \mathbf{z}_{\text{obs}}|. \quad (6)$$

*Estimation of the Macrocycle Distortion Energy.* For small displacements (harmonic approximation), the total macrocyclic distortion energy is simply the sum of energy terms for each of the out-of-plane normal-mode coordinates. In terms of the displacements  $d_k$ , the total distortion energy is given by

$$V_{\text{oop}} = \sum_{k=1}^6 V_{\text{oop}}(d_k) = 2\pi^2 c^2 \sum_{k=1}^6 \tilde{\nu}_k^2 \mathbf{Q}_k^2 = \sum_{k=1}^6 K_k d_k^2. \quad (7)$$

$\mathbf{Q}_k$  is the root-mass-weighted normal coordinate,  $\tilde{\nu}_k$  (in  $\text{cm}^{-1}$ ) is the vibrational frequency of the  $k$ th mode, and  $c$  is the speed of light. The force constant,  $K_k$  (in  $\text{kJ mol}^{-1} \text{Å}^{-2}$ ), is associated with the distortion energy for a 1-Å displacement in the non-mass weighted coordinate system. The force constant depends on the square of the vibrational frequency and, to a lesser extent, on the atomic masses. Using the molecular-mechanics-derived frequencies for the copper-macrocycle reference structure, the energies for a 1-Å deformation are 9.1 (*sad*), 16.5 (*ruf*), 41.3 (*dom*), 67.3 (*wav*), and 238.4  $\text{kJ mol}^{-1}$  (*pro*), respectively.<sup>5,12</sup> For example, the approximately

1-Å ruffling of the heme in cytochrome *c* requires approximately  $16.5 \text{ kJ mol}^{-1}$  be supplied by the protein for this purpose.

From the energies of deformation, it is clear that the perturbation energy causing the macrocyclic distortion (for example, protein interactions or steric crowding interactions between bulky substituents at the porphyrin periphery) can be most easily channeled into the *sad* and *ruf* deformations, less easily into the *dom* and *wav* deformations, and almost never into the *pro* deformation. However, the actual deformations observed depend on not only on the energy but also on how effectively a particular normal deformation is in relieving the perturbing interaction. This is seen most clearly in the X-ray crystal structures of symmetric tetra-substituted porphyrins, for which a nearly pure out-of-plane displacement along only one of the lowest-frequency normal coordinates (*ruf*) is commonly observed.<sup>8,12</sup> Although it is easier to distort along the *sad* coordinate, the *ruf* coordinate more effectively relieves the peripheral steric strain and is the favored distortion mode.

Pure displacements along one of the lowest-frequency normal coordinates give the frequently observed ruffled, saddled, and domed distortions, illustrated in Figure 3.<sup>8</sup> Significant distortions along the *wav* and *pro* coordinates are seen rarely because the energy required to induce a unit distortion along a particular normal coordinate goes up as the square of the frequency of the mode  $K_k$ . Thus, the distortion energy, in this case provided by the steric repulsion of the peripheral substituents, is apparently too small to induce *pro* distortion large enough to show up in the X-ray crystal structures. In particular, this explains why the *pro* deformation is almost never required in the sum of Eqn. (1). That is, this deformation usually requires too much energy to contribute significantly to the observed macrocycle distortion because of the high frequency of this mode.

While the NSD method using this minimal basis of normal deformations is found to sufficiently characterize the heme distortions of the proteins, the *simulated* structures significantly deviate from the *observed* structures for the high-resolution X-ray crystal data of synthetic metalloporphyrins.<sup>12,16</sup> In this case, an essentially exact simulation is obtained for the out-of-plane distortion by using a basis set of deformations expanded to include the second lowest-frequency normal coordinate of each symmetry type (extended basis). The high resolution of X-ray structures of the synthetic porphyrins apparently allow the small contributions from these higher frequency normal deformations to be detected. A discussion of the mathematical procedure for the complete (in-plane and out-of-plane) normal structural decomposition, a discussion of the limits for using the minimal basis set, and the application of NSD to the analysis of synthetic porphyrin crystal structures and protein-bound porphyrin structures is given elsewhere.<sup>5,12</sup>

*Molecular Mechanics Calculations of Heme Structure.* Molecular mechanics calculations will be used to identify and quantify the interactions between the heme and the protein that give rise to the nonplanar distortions. A good example is the cytochromes *c*<sub>3</sub> for which very different structures are observed for the four hemes (Figure 7). Specifically, why are hemes 1 predominantly ruffled, while hemes 4 are saddled (except for the Norway strains)? This question can be addressed at several levels by molecular mechanics. The simplest calculation is to freeze the protein component in place at the X-ray structure positions and let the hemes relax in the protein environment. Does this give the observed contributions of the normal deformations to the heme structure or not? A more intensive calculation is to energy optimize the entire heme protein, and then compare the heme structures given by X-ray crystallography and the calculations. This is easily within the computational limits of our new R10000 SGI workstation. Again, does the calculated structure agree with the X-ray structure? Using such calculations coupled with NSD analysis, specific strong van-der-Waals, H-bond, and electrostatic interactions between the heme and protein can be located. Further calculations can be performed in which individual interactions are turned off to evaluate their influence on the structure of the heme.

Similarly, segments of the protein surrounding the heme can be removed systematically to determine their

influence on the structure of the heme. For the cytochromes *c*, a specific pentapeptide segment is thought to be involved in causing the distortion, so the heme and this protein segment can be energy optimized to determine the predicted structure. The segment length can be varied and specific interactions can be turned on or off to determine their influence on heme structure. Specifically, interactions between the heme and protein and within the protein component itself, *e.g.*, H-bonding in the peptide backbone, H-bonding to the propionic acid substituents, axial coordination to the iron, can be systematically "turned off" in the calculations to determine their individual contributions to the observed nonplanar distortion. As an example, Figure 12 shows the effect on the macrocycle of turning off the covalent attachments of the protein to the porphyrin periphery and to the iron atom of the heme-pentapeptide.

Finally, point mutations of the protein can be investigated by comparing the energy-optimized structures (starting from the X-ray structure) of the wild-type and mutant proteins. Of initial interest for the cytochromes *c* are the mutants of the residues X and Y in the pentapeptide Cys-X-Y-Cys-His. In fact, there is natural variation of the residue X; this residue is Ser for primates and birds, Leu or Gln for yeast, and Ala for other species including horse. There is no X-ray structure for the Cyt-*c* of the birds and primates, but the structures of yeast isozymes 1 (X=Leu) and 2 (X=Gln) are known as are the structures of tuna, horse and rice. Thus, in comparison with the other known X-ray structures (*e.g.*, tuna, horse) which all have Ala for X, one would expect the largest difference for isozyme 2 (Ala to Gln), since the Ala to Leu (iso1) modification is conservative. NSD results indeed show significant differences between isozyme 2 (shown in Figure 2) and the other species available (albacore, rice, horse; Figure 4). In particular, the negative *sad* deformation for these proteins becomes small and positive for isozyme 2 and the *x*- and *y*-*wav* distortions become larger for iso2. The heme conformations in the mutants and natural variants can be calculated and structurally analyzed using NSD; the calculation results can then be compared to the NSD results obtained from crystal structures. In this way, various structural mechanisms giving rise to the observed heme distortions can be detected and evaluated. The calculated structures will also be a useful aid in interpreting the resonance Raman data for the mutant proteins.

Similarly, the distortions caused by varying the apoprotein can be analyzed in terms of the normal deformations produced. In addition, the sign and magnitudes of the normal deformations for the calculated structures can be compared to the normal deformations observed for the hemes in crystal structures. For example, Figure 13 shows the NSD results for the energy-optimized structure for FeMP-11 taken from tuna and horse proteins and for the X-ray structure of the corresponding cytochromes *c*. The agreement is reasonably good except for the *sad* contribution. Here, only small differences in the calculated structure are found because the sequence differences are not in the crucial pentapeptide unit. Our initial efforts will focus on molecular modeling of the *c*-type cytochromes and, specifically, the determination of the structural mechanism of the *ruf* and *sad* deformations.

Mutations will be chosen to test the proposed structural mechanisms. Structures of the mutant proteins calculated using molecular mechanics will be analyzed by NSD to determine whether the mutation influences the heme conformation in the expected way. The results of these calculations will be compared with resonance Raman data on the corresponding mutant proteins supplied by collaborators Hildebrandt and Mauk and the published X-ray structures of Prof. G. Brayer.

Subsequent investigations of this type will focus on the peroxidases, since these proteins exhibit the largest heme distortions in the absence of covalent attachments at the heme periphery. As for the cytochromes *c*, calculated structures of the mutants will be compared using NSD to determine which point mutations influence the heme conformation. The mutants will be especially important for the peroxidase studies, because the specific interactions causing the heme distortion are most likely distributed and consequently will be difficult to locate. The theoretical predictions will be validated by Raman studies of the corresponding mutants of cytochrome *c*

peroxidase supplied by Prof. J. Satterlee. The molecular modeling calculations will be performed by the PI and other UNM personnel using facilities at UNM/Sandia. We now give a brief description of the molecular modeling methods to be employed.

*Molecular Mechanics Methods and the Porphyrin Force Field.* Classical molecular mechanics calculations have previously been used for predicting porphyrin structures by our group,<sup>7,8,22,24</sup> and others including Munro,<sup>38</sup> Marques,<sup>39</sup> and Kollman.<sup>40</sup> The molecular energy-optimization calculations will be performed using POLYGRAF software (Molecular Simulations) and a hybrid force field based on the DREIDING II force field parameters.<sup>41</sup> Specifically, the DREIDING II force field has been modified to include atom types specific to the porphyrin macrocycle.<sup>9a</sup> Force constants for the macrocycle atom types were obtained from normal coordinate analyses of nickel porphyrins.<sup>42</sup> The equilibrium bond lengths and some bond angles were then varied so that the energy-optimized structure of Ni(II) octaethylporphyrin (NiOEP) obtained using the extended DREIDING force field matched the planar crystal structures of NiOEP as closely as possible. DREIDING II parameters were used for all of the nonbonding interactions and for the internal force field of the peripheral substituents of the porphyrin. An improved force field will be used in this work. In this force field, (1) torsions for resonance atom types exocyclic to aromatic ring systems are reduced to 40 % of the value internal to the ring for consistency with DREIDING II,<sup>41</sup> (2) an exponential-6 van-der-Waals functional form is used for the hydrogen atoms,<sup>14</sup> and (3) DREIDING II parameters are consistently used instead of a hybrid of DREIDING I and DREIDING II parameters.<sup>8</sup> Also, a minor error in the counting of the nonbond interactions of the atoms bonded to the metal has been corrected in the POLYGRAF code. Finally, the solvent dielectric constant was set to that of CS<sub>2</sub> (2.64). After these changes, the force field bond distances and angles of the macrocycle were re-optimized by least squares methods<sup>43</sup> to match the planar NiOEP crystal structures. These are minor corrections, and the calculated porphyrin structures differ negligibly from those obtained with the force field used in our previous work. However, significantly improved conformational energies are obtained using this revised force field.

The most important change in the new force field is that the previously used out-of-plane force constants have been reduced by 50%.<sup>16</sup> The 50 % value for reducing the out-of-plane force field was arrived at by requiring that an index set of nonplanar porphyrin structures be accurately predicted. We varied the uniform percent reduction of the out-of-plane force constants of Li *et al.*<sup>42a</sup> in 5 % increments until all structures in the index set were predicted correctly. The index set included a group of several porphyrin crystal structures for which previous versions of the force field predicted either incorrect conformations or degrees of distortion. The set includes NiOEP (planar and *ruf* conformers), NiTPP (planar and *ruf*), Ni 5,15-diphenyl porphyrin (planar and *ruf*), Ni 5,15-dipropylporphyrin (*gab*), Ni 5,15-di-tert-butylporphyrin (*gab*), free base dodecaphenylporphyrin-F<sub>28</sub> (*wav*), and Ni tetra-isopropylporphyrin (*ruf*). For example, for NiOEP and NiTPP, only the planar conformer was predicted with the previous version of the force field; now with the new force field both planar and *ruf* conformers are predicted, with relative energies that are consistent with the equilibrium mixture of the conformers observed in solution studies.<sup>7,16,22,24,27</sup>

Other than the success of the new force field in correctly predicting the structures in the index set, considerations that are more fundamental suggest that this change in the force field is reasonable. Direct incorporation of the out-of-plane force constants<sup>42a</sup> with the in-plane force constants<sup>42c</sup> to arrive at a molecular mechanics force field is known to be a faulty approach in this case. This is because the out-of-plane normal coordinate analysis<sup>42a</sup> was performed independently of the in-plane normal coordinate analysis.<sup>42c</sup> Moreover, it is known that the in-plane force constants contribute to the out-of-plane force field because bonds are stretched for out-of-plane distortions. Thus, when the out-of-plane force constants, obtained independently of these in-plane contributions, are simply added to the in-plane force constants, then we expect the out-of-plane restoring forces will be over estimated. Consequently, previous extensive comparisons of calculated and experimental structures have shown a propensity for the previous version of the force field to underestimate the degree of nonplanarity.

The 50 % reduction in the independently determined force constants corrects this problem in an approximate manner. The new force field greatly improves the ability of the calculations to correctly predict the degree of nonplanarity and the relative energies of various conformers of porphyrins.<sup>16</sup>

*INDO/s molecular orbital calculations.* Quantum mechanical calculations will be carried out using the INDO/s semi-empirical method developed and optimized for spectroscopic predictions by Zerner and coworkers,<sup>44</sup> and various *ab initio* methods such as Gaussian, QUEST, and NWCHEM. The HyperChem (Hypercube, Inc.) program has been used by us extensively for INDO/s calculations. The parameter  $\beta(d)$  in the INDO/s program was varied to give reasonable energies for the d-d transitions for nickel porphyrins and a value of 32 eV was chosen.<sup>8</sup> A convergence limit of  $10^{-7}$  is used. Molecular structures used in the semiempirical calculations are those obtained from molecular mechanics calculations. The quantum-chemical calculations are performed on the entire molecule including the substituents. In addition, for comparison, INDO calculations are often performed on molecular analogs for which the macrocyclic structure is the same as that calculated by molecular mechanics for the entire molecule, but the actual substituents are replaced by methyl groups. As expected, *ab initio* methods give much more reasonable relative energies for the stable conformers than INDO.

*Experimental Studies of Natural Variants, Mutants, and Modified Proteins.* Resonance Raman Spectroscopy. All of these investigations will use resonance Raman spectroscopy to probe the nonplanar distortion of the macrocycle. Resonance Raman spectroscopy is an increasingly useful technique for the characterization of the structural features of hemes in proteins.<sup>30</sup> Various Raman lines are known to be sensitive to structural features such as oxidation and spin state,<sup>30</sup> axial coordination,<sup>30,28</sup> and heme substituents such as the propionates and thioether linkages.<sup>28,46</sup> Of particular interest for out-of-plane heme distortions are the Raman lines  $\nu_8$ ,  $\nu_4$ ,  $\nu_3$ ,  $\nu_2$ , and  $\nu_{10}$ , which show well-characterized<sup>8,14,16,21-23</sup> shifts in frequency as the macrocycle saddles or ruffles. In fact, resonance Raman spectroscopy is the only method that currently can detect the equilibrium mixture of planar and nonplanar conformers that coexist in solution for Ni porphyrins. This mixture has been observed for NiOEP,<sup>3,24,25</sup> NiTPP,<sup>27</sup> Ni meso-(NO<sub>2</sub>)OEP,<sup>7</sup> NiProtoP,<sup>3</sup> Ni uroporphyrin,<sup>3</sup> and the Ni-reconstituted hemoglobin  $\alpha$ -subunits.<sup>3</sup> In some cases, Raman spectroscopy has been used to determine thermodynamic parameters for this equilibrium.<sup>22,27</sup> The lines  $\nu_8$  and  $\nu_{10}$  have been particularly useful measures of the nonplanarity of heme peptides.<sup>28</sup> Except for the cytochrome *c* mutants, all resonance Raman spectroscopy will be performed at UNM.

*Species Variation.* A number of hemoproteins isolated from different species are available commercially or through collaborations. These will be investigated by resonance Raman spectroscopy to determine the influence of natural variation in the amino acid sequence on the heme conformation. For example, pigeon, horse, and tuna cytochromes *c* are available commercially and purified yeast cytochrome *c* isoenzymes are available from Profs. James Satterlee and Jane Vanderkooi. Proteins from these species cover the complete range of variation of the amino acid residues between the cysteines for the cytochromes *c*. These proteins will be investigated by resonance Raman spectroscopy to determine the influence of the side chain at position 15, the only locus of natural sequence variation. Molecular modeling and NSD analysis will aid in interpreting the Raman results. The Raman spectroscopy and modeling will be performed at UNM.

*Mutant Proteins.* We will collaborate with other research groups to obtain resonance Raman spectroscopic data for relevant engineered mutants to test the structural mechanisms of heme distortion and to relate heme structures to biological function. Resonance Raman spectroscopy of yeast isoenzyme cytochrome *c* mutants (as provided by Prof. A. Grant Mauk, at the University of British Columbia, Vancouver) will be carried out in the laboratory of Prof. Peter Hildebrandt at the Max-Planck-Institut für Strahlenchemie, Mülheim a.d. Ruhr. Prof. Hildebrandt has agreed to provide us with the resonance Raman spectroscopic data and to design the experiments in tight collaboration with our group. Special attention will be paid to a detailed analysis of line

shapes for the lines that are most sensitive to macrocycle structure. These Raman studies will be coupled with molecular mechanics calculations for the mutants performed at UNM. NSD will be used to analyze the molecular mechanics structures.

Prof. James Satterlee has agreed to collaborate on studies of the origin of the large, mainly saddling distortion observed in the peroxidases. His group will provide mutants of yeast cytochrome *c* peroxidase (see attached letter) for resonance Raman spectroscopy to be performed in our lab at the Advanced Materials Laboratory at UNM. Prof. Satterlee has developed a very high expression system for virtually any mutant. The required purification steps have been reduced to just 2 days following lysis of the *E. coli* cells in which they are grown whereas the previously published purification required 8 days. His group is currently cloning cytochrome *c* peroxidase into a pET29a system so that the purification can be further simplified into 1 step using the histag method. We expect the Raman studies of the mutants to begin in the second year, but molecular modeling of the mutants will precede the experimental work.

**Modified Proteins.** We will collaborate with Prof. Jane Vanderkooi at the University of Pennsylvania on studies of modified proteins to test the structural origins of nonplanar heme conformations. Initially, digestion products of cytochromes *c* will be investigated including MP-8 and MP-11 and their metal-reconstituted derivatives. The H-65 protein is another possibility. The metal derivatives allow us to control axial ligation and to determine the influence of the size of the metal on nonplanarity. NiMP-11 has already been prepared and preliminary resonance Raman and absorption spectra were obtained in the presence and absence of detergent and at a wide range of pH values. The modified proteins will be prepared at the University of Pennsylvania; Raman and UV-visible spectra will be obtained at UNM/Sandia. Low-spin Ni(II) is small and therefore favors deformations like *ruf* and *sad* which contract the metal core and consequently shorten the metal-nitrogen(pyrrole) bonds. Other metal derivatives, including the Cu, Co, and Zn, will also be prepared. These modified proteins and the native iron derivative will be investigated with resonance Raman spectroscopy, UV-visible absorption spectroscopy, and other experimental techniques as needed.

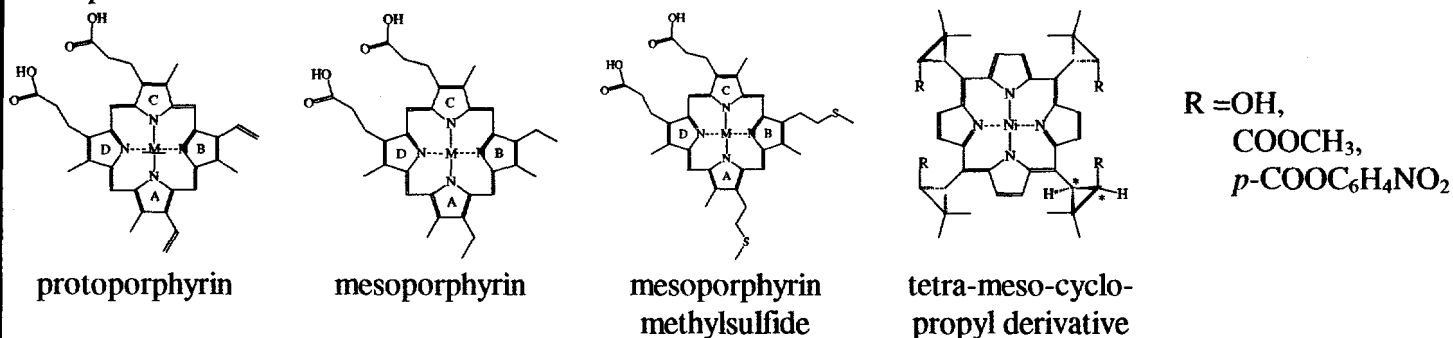
FeMP-11 does not show a splitting of the doubly-degenerate Q-absorption band at low temperature, but the cytochromes *c* do.<sup>45</sup> Assuming that this splitting arises from the breaking of the *x*- and *y*-symmetry of the porphyrin, the heme in cytochrome probably undergoes an additional distortion not evident in the calculated MP-11 structures, and further this additional distortion must break the four-fold symmetry. For example, either a pure *ruf* or a pure *sad* deformation results in  $D_{2d}$  macrocyclic symmetry, retaining the *x*- and *y*-degeneracy. On the other hand, a mixture of the *ruf* and *sad* deformations gives  $S_4$  macrocyclic symmetry, which splits the  $Q_x$  and  $Q_y$  transitions. In this respect, it is interesting that the crystal structures of the cytochromes, which are predominantly *ruf*, also show a strong *sad* component that is not evident in the calculated FeMP-11 structures (Figure 13). Low-temperature absorption and resonance Raman spectroscopy may together be able to conclusively determine the types of deformation and the mechanism of splitting of the Q band of cytochromes *c*.

Some other related questions<sup>45</sup> for the heme peptides will be addressed in our resonance Raman studies. For example, what is the nature of the two distinct forms of CuCyt-*c* that are isolated after metal insertion? Also, what is the nature of the porphyrin derivative formed during the preparation of CuCyt-*c* using the HF prep? This derivative could provide a useful model that is intermediate between the full pentapeptide and model porphyrins such as mesoporphyrin.

**Protein Folding.** Solution conditions such as pH and ionic strength will be varied to vary the protein structure while using Raman spectroscopy to measure the effect of these factors on the conformation of the heme. In addition, the complex interaction of the heme-protein fragments with detergents will be investigated, especially with regard to heme distortion. Experiments with unfolding agents like guanidinium ion and DMSO

will further elucidate the relationship between protein folding and heme conformation. The protein folding studies will be done for both the native and modified proteins, including the heme-peptide fragments like MP-11. At a minimum, these resonance Raman studies will uniquely probe the changes occurring at the active site as the protein unfolds and refolds by monitoring the conformation of the prosthetic group.

**Model Porphyrin Studies.** Model porphyrins will be synthesized by Dr. Michiko Miura at Brookhaven National Laboratory, and Dr. Craig Medforth at the University of California at Davis, through an ongoing collaboration with Prof. Kevin Smith. The model porphyrins will be chosen for the purposes of determining distortion mechanisms, finding spectral markers of deformation type, and evaluating structure-reactivity relationships. Of course, the simplest model for the heme in the cytochromes *c* is Fe mesoporphyrin. Preliminary studies by our group indicate that the structural heterogeneity of Ni mesoporphyrin is similar to that of NiProtoP. This will be determined conclusively and will quantify the effect of reduction of the vinyl groups of the heme on its nonplanar distortion in solution.



We will also attempt to introduce large substituent groups at the vinyl positions to see if there are steric effects on planarity. A dimethylsulfide derivative or a cysteine derivative formed by reducing the vinyl groups would be useful. Again, special attention will be paid to the Raman lines that are sensitive to macrocyclic structure. The interpretation of the spectroscopic results will be supported by molecular mechanics calculations combined with NSD analysis of the resulting structures.

Model synthetic porphyrins which constrain the macrocyclic distortion to a pure deformation along only one normal coordinate are remarkably hard to realize, with the exception of the *ruf* deformation. This conclusion is not obvious, but comes from our preliminary attempts to design symmetrically substituted porphyrins in a purely domed lowest-energy conformation. Nonetheless, model porphyrins that conform to each of the normal deformations shown in Figure 3 are needed to help develop spectroscopic markers for the different types of distortion. Strained, capped porphyrins would seem to be an obvious way to generate a purely domed porphyrin, but molecular mechanics calculations show that contributions from other normal deformations are present because of the symmetry properties of the porphyrin substituent groups. At present, the meso-tetra-cyclopropylporphyrin derivative seems to be the best hope for a porphyrin possessing an almost purely domed lowest-energy conformation. Even in this case, the domed conformer must be stabilized by H-bonding of the  $R = \text{OH}$  groups to perfluorocyclobutane in a 1:1 complex. Further efforts will be made to design, synthesize, and structurally characterize porphyrins whose lowest-energy conformations are specific, pure normal deformations. Modeling and resonance Raman spectroscopy of the resultant models will be done by our group at UNM.

**Structure-Function Relationships.** We will first complete our investigation of the effects of nonplanar distortions on the axial ligand affinity of nickel porphyrins. At present, this work is restricted to the effect of ruffling on affinity because of our use of the *meso*-tetraalkylporphyrins (see Preliminary Results section). An interesting follow-on to this work will be an investigation of the 5,15-dialkylporphyrins. The lowest-energy conformation of the dialkylporphyrins is composed of a mixture of the *ruf* and *dom* deformations. The effect of

the introduction of the *dom* deformation on ligand affinity will be determined by comparison with the tetraalkylporphyrin results.

A study of the series of nickel dialkylporphyrins would allow us to address another issue as well. For the tetraalkylporphyrin, axial ligation could induce a conformational change from a *ruf* to a *dom* conformer. This is possible because axial coordination can result in the *dom* conformer becoming lower in energy than the *ruf* conformer.<sup>47</sup> For the tetra-substituted porphyrins, there is a barrier between these two conformers. This is not the case for the di-substituted porphyrins, which admit a continuously variable mixture of the *dom* and *ruf* deformations. Thus, a comparative study of these two series of porphyrins could be informative as to the consequences of energy barriers between conformers.

Axial ligand binding to iron porphyrins is more complicated than that for Ni porphyrins because of the involvement of more metal d orbitals in ligation, especially the  $d_x$  orbitals. Nevertheless, out-of-plane distortions are expected to have consequences for axial coordination of both exogenous and endogenous ligands of the heme proteins. Model iron porphyrins, with known macrocyclic deformations and ligand orientations, will be studied using vibrational spectroscopy to measure the influence of the various types of deformations on axial coordination to Fe in various oxidation and spin states. The spectroscopic results will be coupled with molecular modeling and NSD analysis to fully elucidate the effects of axial ligation to Fe. Binding of both  $\sigma$  and  $\pi$  axial ligands will also be investigated.

One area in which a connection between hemoprotein function and heme structure might be made is in explaining the relative affinities of CO and O<sub>2</sub> in hemoglobin and myoglobin. Encumbered heme model compounds have been synthesized to force the Fe-CO unit to adopt a bent geometry reported for myoglobin, and to examine the consequences of this geometry upon reactivity.<sup>4,48</sup> This bent binding geometry has been invoked in order to explain the altered relative affinities of CO and O<sub>2</sub> in the hemoproteins. That is, by forcing a bent geometry on the CO ligand, its affinity is reduced with respect to the unencumbered heme, whereas the affinity of O<sub>2</sub>, which prefers the bent geometry, is unaltered. Surprisingly, the crystal structures of some models indicate that the mechanism may also involve a ruffling distortion of the porphyrin ring instead of the expected bending of the Fe-C-O unit.<sup>22</sup> Combined structural and ligand-binding studies for a series of porphyrins in know deformations of differing magnitude will help to define the effects of macrocyclic structure on O<sub>2</sub> and CO binding. For the capped porphyrin model compounds, the heme distortion may merely relieve steric interaction with the ligand, but there may also be a direct effect of heme conformation on ligand affinity. Molecular modeling will also be employed to address this problem.

Another interesting possibility is that of conformational trapping of excited states. Nickel porphyrins are known to undergo an electronic transition that changes the metal d-orbital populations.<sup>49</sup> The  $d_{z^2}^2 \rightarrow d_{z^2}^1, d_{x^2-y^2}^1$  transition results in a large change in the effective metal size. This change in the optimal metal-nitrogen(pyrrole) bond length favors some normal deformations and disfavors others. See Figure 15. In particular, the *ruf* and *sad*

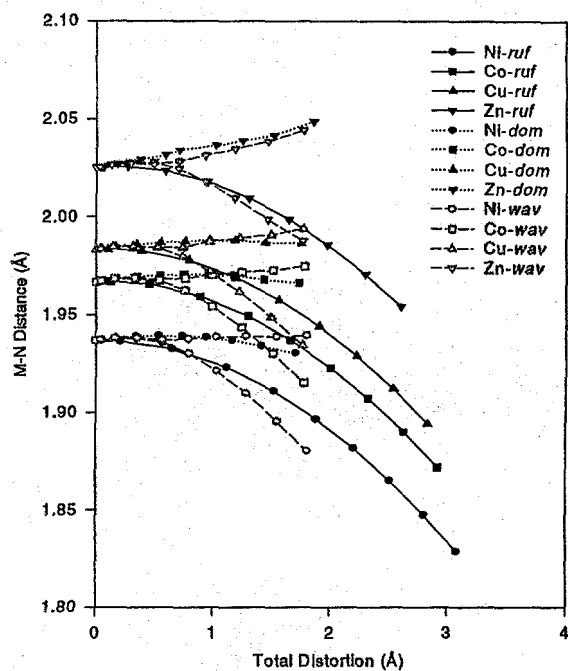


**Figure 15.** Effect of different out-of-plane normal deformations on the metal-nitrogen bond distance for different metals. Ruffling drastically shortens the M-N distance, while doming slightly increases it. The wav(x) deformation shorten the M-N bonds in one direction and slightly lengthens the bonds in the orthogonal direction. Saddling (not shown) shortens the M-N bond distance. Results are from molecular mechanics calculations and NSD analyses.

deformations, which drastically reduce the optimal core size of the porphyrin, are disfavored by this d-d transition. In contrast, the *dom* deformation actually slightly increases the optimal core size and thus favors this d-d transition. The outcome of these structural considerations is that it is possible that the d-d electronic transition could result in a different stable conformer becoming the lowest energy conformer. Therefore, the electronic transition could induce a conformational change. Furthermore, if there is a barrier between the two conformers, as is the case for the *dom* and *ruf* conformer of the tetra-substituted porphyrins, then the conformational barrier may trap the excited state, *i.e.*, increase its lifetime.<sup>8,50</sup> On the other hand, if no barrier exists between the two conformers (*e.g.*, two conformers differing in the relative amounts of doming and ruffling)<sup>16</sup>, then conformational trapping of the excited state would be less likely to occur. We will investigate conformational trapping of the excited state of tetra(*meso*-*tert*-butyl)porphyrin and other tetra-substituted porphyrins in collaborations with other workers using ultrafast spectroscopic techniques.

The computational and experimental studies described cover the entire range of goals outlined in the specific aim section. Successful completion of these challenging experiments and calculations are feasible and realistic given four or five years of stable funding at the level requested.

e. Human Subjects

Not Applicable.

f. Vertebrate Animals.

Not Applicable.

g. Literature Cited.

1. (a) "Structural and Theoretical-Models of Photosynthetic Chromophores: Implications for Redox, Light-Absorption Properties and Vectorial Electron Transfer" Barkigia, K. M.; Chantranupong, L.; Smith, K. M.; Fajer, J., *J. Am. Chem. Soc.* **1988**, *110*, 7566-7567. (b) "Structure and X-ray Amino-Acid-Sequence of a Bacteriochlorophyll-A Protein From *Prosthecochloris Aestuarii* Refined at 1.9 Å Resolution" Tronrud, D. E.; Schmid, M. F.; Matthews, B. W., *J. Mol. Biol.* **1986**, *188*, 443-454. (c) "Structural Consequences of Nickel Versus Macrocycle Reductions in F430 Models: EXAFS Studies of a Ni(I) Anion and Ni(II)  $\Pi$ -Anion" Furenlid, L. R.; Renner, M. W.; Smith, K. M.; Fajer, J., *J. Am. Chem. Soc.* **1990**, *112*, 1634-1635. (d) "EXAFS Studies of Nickel(II) and Nickel(I) Factor-430M: Conformational Flexibility of the F430 Skeleton" Furenlid, L. R. Renner, M. W.; Smith, K. M.; Fajer, J., *J. Am. Chem. Soc.* **1990**, *112*, 8987-8989. (e) "Why Does Nature Not Use the Porphyrin Ligand in Vitamin-B12" Geno, M. K.; Halpern, J., *J. Am. Chem. Soc.* **1987**, *109*, 1238-1240.
2. "Structural Changes in Cytochrome *c* upon Hydrogen-Deuterium Exchange" Hildebrandt, P.; Vanhecke, F.; Heibel, G.; Mauk, A. G., *Biochemistry* **1993**, *32*, 14158-14164.
3. "Influences of  $\pi$ - $\pi$  Complex Formation, Dimerization, and Binding to Hemoglobin on the Planarity of Nickel(II) Porphyrins" Alden, R. G.; Ondrias, M. R.; Shelnutt, J. A., *J. Am. Chem. Soc.* **1990**, *112*, 691-697.
4. (a) "Dioxygen and Carbon Monoxide Binding to Apolar Cyclophane Hemes: Durene-Capped Hemes" David, S.; James, B. R.; Dolphin, D.; Traylor, T. G.; Lopez, M. A., *J. Am. Chem. Soc.* **1994**, *116*, 6-14. (b) "Structure-Reactivity Relationship in Oxygen and Carbon-Monoxide Binding with Some Heme Models" Tetreau, C.; Lavalette, D.; Momenteau, M.; Fischer, J.; Weiss, R. *J. Am. Chem. Soc.* **1994**, *116*, 11840-11848.
5. "Conformation of the Porphyrin Macrocycle Is Conserved in Hemoproteins of the Same Functional Class" Jentzen, W.; Shelnutt, J. A., *J. Am. Chem. Soc.* **1997**, in press.
6. "Conserved Nonplanar Heme Distortions in Cytochromes *c*" Hobbs, J. D.; Shelnutt, J. A., *J. Protein Chem.* **1995**, *14*, 19-25.
7. "Planar-Nonplanar Conformational Equilibrium in Metal Derivatives of Octaethylporphyrin and meso-Nitrooctaethylporphyrin" Anderson, K. K.; Hobbs, J. D.; Luo, L.; Stanley, K. D.; Quirke, J. M. E.; Shelnutt, J. A., *J. Am. Chem. Soc.* **1993**, *115*, 12346-12352.
8. "Ruffling in a Series of Nickel(II) meso-Tetrasubstituted Porphyrins as a Model for the Conserved Ruffling of the Heme of Cytochromes *c*" Jentzen, W.; Simpson, M. C.; Hobbs, J. D.; Song, X.; Ema, T.;

- Nelson, N. Y.; Medforth, C. J.; Smith, K. M.; Veyrat, M.; Mazzanti, M.; Ramasseul, R.; Marchon, J.-C.; Takeuchi, T.; Goddard, III, W. A.; Shelnutt, J. A., *J. Am. Chem. Soc.* **1995**, *117*, 11085-11097.
9. (a) "Relationships between Structural Parameters and Raman Frequencies for Some Planar and Nonplanar Nickel(II) Porphyrins" Shelnutt, J. A.; Medforth, C. J.; Berber, M. D.; Barkigia, K. M.; Smith, K. M., *J. Am. Chem. Soc.* **1991**, *113*, 4077-4087. (b) "Tetracycloalkenyl-meso-tetraphenylporphyrins as Models for the Effect of Non-Planarity on the Light Absorption Properties of Photosynthetic Chromophores" Medforth, C. J.; Berber, M. D.; Smith, K. M.; Shelnutt, J. A., *Tetrahedron Lett.* **1990**, *31*, 3719-3722.
10. (a) "Multiple Four-Coordinate Forms in a Nickel Hydrocorphinate Related to Cofactor F430 of Methylreductase" Shelnutt, J. A., *J. Phys. Chem.* **1989**, *93*, 6283. (b) "Structural and Spectroscopic Characterization of Exogenous Ligand Binding to Isolated Factor F430 and Its Configurational Isomers" Shiemke, A. K.; Kaplan, W. A.; Hamilton, C. L.; Shelnutt, J. A.; Scott, R. A., *J. Biol. Chem.* **1989**, *264*, 7276-7284. (c) "Coordination Chemistry of F430" Shiemke, A. K.; Shelnutt, J. A.; Scott, R. A., *J. Biol. Chem.* **1989**, *264*, 11236-11245. (d) "Axial Ligation-Induced Changes in Nickel Hydrocorphinoids Related to Coenzyme F430 Detected by Raman Difference Spectroscopy" Shelnutt, J. A., *J. Am. Chem. Soc.* **1987**, *109*, 4169-4173. (e) "Photodynamics of a Nickel Hydrocorphinoid Model of F430" Crawford, B. A.; Findsen, E. W.; Ondrias, M. R.; Shelnutt, J. A., *Inorg. Chem.* **1988**, *27*, 1842-1846. (f) "Resonance Raman Spectroscopic Investigation of Axial Coordination of *M. thermoautotrophicum* Methyl Reductase and its Nickel Tetrapyrrole Cofactor F430" Shiemke, A. K.; Scott, R. A.; Shelnutt, J. A., *J. Am. Chem. Soc.* **1988**, *110*, 1645-1646.
11. "Metal Dependence of the Nonplanar Distortion of Octaalkyltetraphenylporphyrins" Sparks, L. D.; Medforth, C. J.; Park, M.-S.; Chamberlain, J. R.; Ondrias, M. R.; Senge, M. O.; Smith, K. M.; Shelnutt, J. A., *J. Am. Chem. Soc.* **1993**, *115*, 581-592.
12. "Structural Characterization of Synthetic and Protein-Bound Porphyrins in Terms of the Lowest-Frequency Normal Coordinates of the Macrocycle" Jentzen, W.; Song, X.-Z.; Shelnutt, J. A., *J. Phys. Chem.* **1997**, in press.
13. "Correlations between Raman Frequencies and Structure for Planar and Nonplanar Metalloporphyrins" Sparks, L. D.; Anderson, K. K.; Medforth, C. J.; Smith, K. M.; Shelnutt, J. A., *Inorg. Chem.* **1994**, *33*, 2297-2302.
14. "Structural Heterogeneity and Coordination Chemistry of Nickel (II) Octaethyl-meso-nitroporphyrins" Hobbs, J. D.; Majumder, S. A.; Luo, L.; Sickelsmith, G. A.; Quirke, J. M. E.; Medforth, C. J.; Smith, K. M.; Shelnutt, J. A., *J. Am. Chem. Soc.* **1994**, *116*, 3261-3270.
15. (a) "Non-planar Distortion Modes for Highly Substituted Porphyrins" Medforth, C. J.; Senge, M. O.; Smith, K. M.; Sparks, L. D.; Shelnutt, J. A., *J. Am. Chem. Soc.* **1992**, *114*, 9859-9869. (b) "A Planar Dodecasubstituted Porphyrin" Senge, M. O.; Medforth, C. J.; Sparks, L. D.; Shelnutt, J. A.; Smith, K. M., *Inorg. Chem.* **1993**, *32*, 1716-1723. (c) "Raman Spectroscopic Characterization of Isomers of Copper and Zinc N-Phenylprotoporphyrin IX Dimethyl Ester" Sparks, L. D.; Chamberlain, J. R.; Hsu, P. Y.-F.; Ondrias, M. R.; Swanson, B.; Ortiz de Montellano, P.; Shelnutt, J. A., *Inorg. Chem.* **1993**, *32*, 3153-3161. (d) "Comparative Analysis of the Conformations of Symmetrically and Asymmetrically Deca- and Undeca-substituted Porphyrins Bearing meso-Alkyl or Aryl Groups" Senge, M. O.; Medforth, C. J.; Forsyth, T. P.; Lee, D. A.; Olmstead, M. M.; Jentzen, W.; Pandey, R. K.; Shelnutt, J. A.; Smith, K.

- M. *Inorg. Chem.* **1997**, in press. (e) "NMR Studies of Nonplanar Porphyrins Part 1. Axial Ligand Orientations in Highly Nonplanar Porphyrins" Medforth, C. J.; Muzzi, C. M.; Shea, K. M.; Smith, K. M.; Abraham, R. J.; Jia, S.-L.; Shelnutt, J. A. *J. C. S., Perkin Trans. II*, **1997**, in press. (f) "NMR Studies of Nonplanar Porphyrins. Part 2. Effect of Nonplanar Conformational Distortions on the Porphyrin Ring Current" Medforth, C. J.; Muzzi, C. M.; Shea, K. M.; Smith, K. M.; Abraham, R. J.; Jia, S.; Shelnutt, J. A. *J. C. S., Perkin Trans. II*, **1997**, in press. (g) "Solution Conformations of Dodecasubstituted Cobalt(II) Porphyrins" Medforth, C. J.; Hobbs, J. D.; Rodriguez, M. R.; Abraham, R. J.; Smith, K. M.; Shelnutt, J. A., *Inorg. Chem.* **1995**, *34*, 1333-1341.
16. "Representation of Nonplanar Structures of Nickel(II) 5,15-Disubstituted Porphyrins in Terms of Displacements along the Lowest-Frequency Normal Coordinates of the Macrocycle" Song, X.-Z.; Jentzen, W.; Jia, S.-L.; Jaquinod, L.; Nurco, D. J.; Medforth, C. J.; Smith, K. M.; Shelnutt, J. A., *J. Am. Chem. Soc.* **1996**, *118*, 12975-12988.
17. (a) Warburg, O., *Ber. Dtsch. Chem. Ges.* **1925**, *58*, 1001-1011. (b) Warburg, O., *Biochem. Z.* **1926**, *177*, 471-486. (c) Warburg, O.; Neglein, E., *Biochem. Z.* **1929**, *214*, 64-100.
18. (a) "Complex Formation between Methionine and a Heme Peptide from Cytochrome *c*" Harbury, H. A.; Cronin, J. R.; Fanger, M. W.; Hettinger, T.P.; Murphy, A. J.; Myer, Y. P.; Vinogradov, S. N., *Proc. Natl. Acad. Sci. U.S.A.* **1965**, *54*, 1658-1664. (b) Dickerson, R. E.; Timkovich, R. in *The Enzymes* (Boyer, P., Ed.) Vol. XI, Academic: New York, 379-492, **1975**. (c) "Coupling between Oxidation State and Hydrogen Bond Conformation in Heme Proteins" Valentine, J. S.; Sheridan, R. P.; Allen, L. C.; Kahn, P. C., *Proc. Natl. Acad. Sci. U.S.A.* **1979**, *76*, 1009-1013. (d) "Cytochrome *c* Models" Mashiko, T.; Marchon, J.-C.; Musser, D. T.; Kastner, M. E.; Scheidt, W. R., *J. Am. Chem. Soc.* **1979**, *101*, 3653-3655. (e) "Influence of Hydrogen Bonding on the Properties of Iron Porphyrin Imidazole Complexes. An Internally Hydrogen Bonded Imidazole Ligand" Quinn, R.; Mercer-Smith, J.; Burnstyn, J. N.; Valentine, J. S., *J. Am. Chem. Soc.* **1984**, *106*, 4136-4144. (f) "Amino-Acid-Sequence, Heme-Iron Coordination Geometry and Functional-Properties of Mitochondrial and Bacterial *c*-type Cytochromes" Senn, H.; Wüthrich, K., *Q. Rev. Biophys.* **1985**, *18*, 111-134.
19. "Metal Substitution in Hemoglobin and Myoglobin" Hoffman, B. M., in *The Porphyrins* Vol. VII Dolphin, D., Ed., (Academic: New York, 1979) pp. 403-444.
20. (a) "High-Resolution Refinement of Yeast Iso-1-Cytochrome-*c* and Comparisons with Other Eukaryotic Cytochromes-*c*" Louie, G. V.; Brayer, G. D., *J. Mol. Biol.* **1990**, *214*, 527-555. (b) "Crystal Structure of Yeast Cytochrome *c* Peroxidase Refined at 1.7-Å Resolution" Finzel, B. C.; Poulos, T. L.; Kraut, J., *J. Biol. Chem.* **1984**, *259*, 13027-13036.
21. "Planar Solid-State and Solution Structures of (Porphinato)nickel(II) As Determined by X-ray Diffraction and Resonance Raman Spectroscopy" Jentzen, W.; Turowska-Tyrk, I.; Scheidt, W. R.; Shelnutt, J. A., *Inorg. Chem.* **1996**, *35*, 3559-3567.
22. "Conformational Properties of Nickel(II) Octaethylporphyrin in Solution. 1. Resonance Excitation Profiles and Temperature Dependence of Structure-Sensitive Raman Lines" Jentzen, W.; Unger, E.; Karvounis, G.; Shelnutt, J. A.; Dreybrodt, W.; Schweitzer-Stenner, R., *J. Phys. Chem.* **1996**, *100*, 14184-14191.

23. "Synthesis and Spectroscopic Characterization of Octaacetic Acid Tetraphenylporphyrins" Miura, M.; Majumder, S. A.; Hobbs, J. D.; Renner, M. W.; Furenlid, L. R.; Shelnutt, J. A., *Inorg. Chem.* **1994**, *33*, 6078-6085.
24. "Ruffling of Nickel(II) Octaethylporphyrin in Solution" Alden, R. G.; Crawford, B. A.; Doolen, R.; Ondrias, M. R.; Shelnutt, J. A., *J. Am. Chem. Soc.* **1989**, *111*, 2070-2072.
25. "Nickel Octaethylporphyrin Ruffling Dynamics from Resonance Raman-Spectroscopy" Czernuszewicz, R. S.; Li, X.; Spiro, T. G., *J. Am. Chem. Soc.* **1989**, *111*, 7024-7031.
26. "Resonance Raman Spectroscopy of Non-Planar Nickel Porphyrins" Shelnutt, J. A.; Majumder, S. A.; Sparks, L. D.; Hobbs, J. D.; Medforth, C. J.; Senge, M. O.; Smith, K. M.; Miura, M.; Luo, L.; Quirke, J. M. E., *J. Raman Spectrosc.* **1992**, *23*, 523-529.
27. "Planar and Nonplanar Conformations of (Meso-Tetraphenylporphinato)nickel(II) in Solution as Inferred from Solution and Solid-State Raman Spectroscopy" Jentzen, W.; Unger, E.; Song, X.-Z.; Turowska-Tyrk, I.; Schweitzer-Stenner, R.; Dreybrodt, W.; Scheidt, W. R.; Shelnutt, J. A., *J. Phys. Chem.* submitted.
28. "Resonance Raman Investigation of Imidazole and Imidazolate Complexes of Microperoxidase: Characterization of the Bis(histidine) Axial Ligation in c-Type Cytochromes" Othman, S.; Le Lirzin, A.; Desbois, A., *Biochemistry* **1994**, *33*, 15437-15448.
29. "Chemistry of Corphinoids" Eschenmoser, A., *Ann. N.Y. Acad. Sci.* **1986**, *471*, 108-129.
30. (a) "The Resonance Raman Spectroscopy of Metalloporphyrins and Heme Proteins" Spiro, T. G., in *Iron Porphyrins* (Lever, A. B. P.; Gray H. B., Eds.) Part II, Addison-Wesley: London, 89-159, 1983. (b) "Resonance Raman-Spectroscopy as a Probe of Heme Protein Structure and Dynamics" Spiro, T. G., *Adv. Protein Chem.* **1985**, *37*, 111-159. (c) Kitagawa, T.; Ozaki, Y., *Struct. Bonding* **1987**, *64*, 71-114. (d) Spiro, T. G.; Li, X.-Y. in *Biological Applications of Raman Spectroscopy* (Spiro, T. G., Ed.) Wiley: New York, 1-37, **1988**. (e) "Resonance Raman-Spectroscopy of c-type Cytochromes" Desbois, A., *Biochimie* **1994**, *76*, 693-707.
31. "Horse Heart Ferricytochrome c: Conformation and Heme Configuration of High Ionic Strength Acidic Forms" Myer, Y. P.; Saturno, A. F., *J. Protein Chem.* **1991**, *10*, 481-494.
32. "New Crystalline Phase of (Octaethylporphinato)nickel(II). Effects of  $\pi$ - $\pi$  Interactions on Molecular Structure and Resonance Raman Spectra" Brennan, T. D.; Scheidt, W. R.; Shelnutt, J. A., *J. Am. Chem. Soc.* **1988**, *110*, 3910-3924.
33. (a) "Dynamic photophysical properties of conformationally distorted nickel porphyrins .1. Nickel(II) dodecaphenylporphyrin" Drain, C.M.; Kirmaier, C.; Medforth, C. J.; Nurco, D. J.; Smith, K. M.; Holten, D., *J. Phys. Chem.* **1996**, *100*, 11984. (b) Holten, D.; Shelnutt, J. A., unpublished results.
34. (a) "Nonplanar Porphyrins: X-Ray Structures of (2,3,7,8,12,13,17,18-Octaethyl-5,10,15,20-Tetraphenylporphinato)Zinc(II) and (2,3,7,8,12,13,17,18-Octamethyl-5,10,15,20-Tetraphenylporphinato)Zinc(II)" Barkigia, K.M.; Berber, M.D.; Fajer, J.; Medforth, C.J.; Renner, M.W.; Smith, K.M., *J. Am. Chem. Soc.* **1990**, *112*, 8851. (b) "Electrochemistry and spectral characterization of oxidized and reduced (TPPBrX)FeCl where TPPBrX is the dianion of  $\beta$ -brominated-pyrrole tetraphenylporphyrin and X varies

- from 0 to 8" Tagliatesta, P.; Li, J.; Autret, M.; Van Caemelbecke, E.; Villard, A.; D'Souza, F.; Kadish, K.M., *Inorg. Chem.* **1996**, *35*, 5570-5576.
35. "Redox Properties and Alkane Oxidation Activity within a Series of Novel Fluorinated Iron(III) Dodecaphenylporphyrins" Camelbeck, E. V.; Forsyth, T. P.; Kadish, K. M.; Medforth, C. J.; Nurco, D. J.; Shelnutt, J. A.; Showalter, M.; Smith, K. M.; D'Souza, F., **1997**, in preparation .
36. "Ligands, Spin State, and Geometry in Hemes and Related Metalloporphyrins" Scheidt, W.R.; Gouterman, M., in *Iron Porphyrins* (Lever, A. B. P.; Gray H. B., Eds.) Part I, Addison-Wesley: London, **1983**, 89-139.
37. "Axial Ligand Orientation in Iron(III) Porphyrinates: Effect of Axial  $\pi$ -Acceptors: Characterization of the Low-Spin Complex  $[\text{Fe}(\text{TPP})(4\text{-CNPY})_2]\text{ClO}_4$ " Safo, M. K.; Walker, F. A.; Raitsimring, A. M.; Walters, W. P.; Dolata, D. P.; DeBrunner, P. G.; Scheidt, W. R., *J. Am. Chem. Soc.* **1994**, *116*, 7760-7770.
38. (a) "A Force Field for Molecular Mechanics Studies of Iron Porphyrins" Munro, O. Q.; Marques, H. M.; Debrunner, P.G.; Mohanrao, K.; Scheidt, W. R. *J. Am. Chem. Soc.* **1995**, *117*, 935. (b) "A Molecular Mechanics Model of the Metalloporphyrins: The Role of Steric Hindrance in Discrimination in Favor of Dioxygen Relative" Munro, O. Q.; Bradley, J.C.; Hancock, R. D.; Marques, H. M.; Marsicana, F. *J. Am. Chem. Soc.* **1992**, *114*, 7218.
39. (a) "A Force Field for Molecular Mechanics Studies of Iron Porphyrins" Marques H. M.; Munro, O. Q.; Grimmer, N. E.; Levendis, D. C.; Marsicano, F.; Patrick, G.; Markonlides, T. *J. Chem. Soc. Faraday Trans.* **1995**, *91*, 1741. (b) "A Molecular Mechanics Model of the Metalloporphyrins: The Role of Steric Hindrance in Discrimination in Favor of Dioxygen Relative to Carbon Monoxide in Some Heme Models" Hancock, R. D.; Weaving, F. S.; Marques, H. M., *J. Chem. Soc., Chem. Commun.* **1989**, 1176-1178.
40. (a) "Computer-Simulation Studies of Spherands, Crowns and Porphyrins : Application of Computer-Graphics, Distance Geometry, Molecular Mechanics and Molecular Dynamics Approaches" Kollman, P. A.; Grootenhuis, D. D. J.; Lopez, M. A. *Pure & Appl. Chem.* **1989**, *61*, 593-596. (b) "Application of Molecular-Dynamics and Free-Energy Perturbation-Methods to Metalloporphyrin Ligand Systems. 1. CO and Dioxygen Binding to 4 Heme Systems" Lopez, M. A.; Kollman, P.A., *J. Am. Chem. Soc.* **1989**, *111*, 6212-6222.
41. "DREIDING: A Generic Force-Field for Molecular Simulations" Mayo, S. L.; Olafson, B. D. ; Goddard, III, W. A., *J. Phys. Chem.* **1990**, *94*, 8897-8909.
42. (a) "Consistent Porphyrin Force-Field. 3. Out-of-Plane Modes in the Resonance Raman-Spectra of Planar and Ruffled Nickel Octaethylporphyrin" Li, X.-Y.; Czernuszewics, R. S.; Kincaid, J. R.; Spiro, T. G. *J. Am. Chem. Soc.* **1989**, *111*, 7012-7023. (b) "Consistent Porphyrin Force-Field .1. Normal-Mode Analysis for Nickel Porphine and Nickel Tetraphenylporphine from Resonance Raman and Infrared Spectra and Isotope Shifts" Li, X. -Y.; Czernuszewics, R. S.; R. S.; Kincaid, J.R.; Su, Y. O.; Spiro, T. G. *J. Phys. Chem.* **1990**, *94*, 31. (c) "Consistent Porphyrin Force-Field .2. Nickel Octaethylporphyrin Skeletal and Substituent Mode Assignments from N-15, Meso-d<sub>4</sub>, and Meso-d<sub>16</sub> Raman and Infrared Isotope Shifts" Li, X. -Y.; Czernuszewics, R. S.; R. S.; Kincaid, J. R.; Stein, P.; Spiro, T. G. *J. Phys. Chem.* **1990**, *94*, 31-47.

43. (a) "Hessian-Biased Force-Fields from Combining Theory and Experiment" Dasgupta, S.; Goddard, W. A., III. *J. Chem. Phys.* **1989**, *90*, 7207-7215. (b) Yamasaki, T.; Dasgupta, S.; Goddard, W. A., III. *J. Phys. Chem.* **1995**, submitted for publication.
44. (a) "An Intermediate Neglect of Differential Overlap Technique for Spectroscopy: Pyrrole and the Azines" Ridley, J. E.; Zerner, M. C. *Theor. Chim. Acta* **1973**, *32*, 111. (b) "An Intermediate Neglect of Differential Overlay Theory for Transition Metal Complexes: Fe, Co and Cu Chlorides" Bacon, A.; Zerner, M. C. *Theor. Chim. Acta* **1979**, *53*, 21. (c) "An Intermediate Neglect of Differential Overlap Technique for Spectroscopy of Transition Metal Complexes. Ferrocene" Zerner, M. C.; Loew, G. H.; Kirchner, R. F.; Mueller-Westerhoff, U. T. *J. Am. Chem. Soc.* **1980**, *102*, 589. (d) "Electronic-Structure and Spectra of Various Spin States of (Porphinato)Iron(III) Chloride" Edwards, W. D.; Weiner, B.; Zerner, M. C. *J. Phys. Chem.* **1988**, *92*, 6188-6197.
45. Vanderkooi, J., personal communication.
46. "Complete Assignment of Cytochrome-*c* Resonance Raman-Spectra Via Enzymatic Reconstitution with Isotopically Labeled Hemes" Hu, S.; Morris, I. K.; Singh, J. P.; Smith, K. M.; Spiro, T. G., *J. Am. Chem. Soc.* **1993**, *115*, 12446-12458.
47. "A Molecular Venus Fly Trap. Induced-Fit Complexation of Pyridine Guests by Flipping of a Zinc(II) Chioroporphyrin Host Triggered by Axial Binding" Mazzanti, M.; Marchon, J.-C.; Shang, M.; Scheidt, W.R.; Jia, S.-L.; Shelnutt, J.A. *Science*, submitted (1997).
48. "Theoretical Study of the Distal-Side Steric and Electrostatic Effects on the Vibrational Characteristics of the Fe-CO Unit of the Carbonylheme Proteins and their Models" Kushkuley, B.; Stavrov, S. S., *Biophys. J.* **1996**, *70*, 1214-1229.
49. (a) "Nickel Porphyrin Photophysics and Photochemistry. A picosecond investigation of ligand binding and release in the excited state" Kim, D.-H.; Kirmaier, C.; Holten, D., *Chem. Phys.* **1983**, *75*, 305-322. (b) "Picosecond measurements on the binding and release of basic ligands by excited states of Ni(II) porphyrins" Kim, D.-H.; Holten, D., *Chem. Phys. Lett.* **1983**, *98*, 584.
50. Holten, D., personal communication.

DISTRIBUTION:

1	MS-0333	A. J. Hurd, 1841
1	MS-0340	M. J. Cieslak, 1831
1	MS-0702	D. E. Arvizu, 6200
1	MS-0710	A. P. Sylwester, 6210
5	MS-0710	J. A. Shelnut, 6210
1	MS-0710	C. Kyle, 6210
1	MS-0710	X.-Z. Song, 6210
1	MS-0710	J.-G. Ma, 6210
1	MS-0710	S.-L. Jia, 6210
1	MS-0710	G. N. Ryba, 6210
1	MS-0710	T. M. Nenoff, 6210
1	MS-0724	J. B. Woodard, 6000
1	MS-0958	C. Adkins, 1472
1	MS-1079	A. D. Romig, 1300
1	MS-1111	G. Heffelfinger, 9225
1	MS-1111	J. D. Hobbs, 9225
1	MS-1349	C. J. Brinker, 1831
3	MS-1349	J. Cesarano, III, 1831
1	MS-1349	W. F. Hammetter, 1846
1	MS-1349	R. E. Loehman, 1808
1	MS-1425	M. W. Scott, 1307
1	MS-1425	S. J. Martin, 1315
1	MS-1436	D. L. Chavez, 4523
1	MS-1800	H. J. Saxton, 1435
1	MS-1802	G. E. Pike, 1434
1	MS-9161	W. G. Wolfer, 8716
1	MS-9214	L. M. Napolitano, 8117
1	MS-9405	J. M. Hruby, 8230
1	MS-0161	Central Technical Files, 8523-2
5	MS-0899	Technical Library, 4414
1	MS-0619	Print Media, 12615
2	MS-0100	Document Processing, 7613-2 For DOE/OSTI